An Introduction to Neural Data Compression

Yibo Yang, Stephan Mandt, and Lucas Theis

Abstract—Neural compression is the application of neural networks and other machine learning methods to data compression. While machine learning deals with many concepts closely related to compression, entering the field of neural compression can be difficult due to its reliance on information theory, perceptual metrics, and other knowledge specific to the field. This introduction hopes to fill in the necessary background by reviewing basic coding topics such as entropy coding and rate-distortion theory, related machine learning ideas such as bits-back coding and perceptual metrics, and providing a guide through the representative works in the literature so far.

Index Terms—Neural compression, variational autoencoders, rate-distortion theory, bits-back coding, image and video compression

✦

1 INTRODUCTION

THE goal of data compression is to reduce the number of bits needed to represent useful information. *Neural*, or *learned* compression, is the application of neural networks and related machine learning techniques to this task. This article aims to serve as an entry point for machine learning researchers interested in compression by reviewing the information theory background as well as the representative methods and techniques in neural compression.

Neural compression draws on a rich history of learning-based approaches to image processing. Indeed, many problems in computational photography can be viewed as lossy image compression; e.g., image super-resolution can be solved by learning a decoder for a fixed encoder (the image downsampling process) [1][2]. In fact, neural networks have been applied to image compression in the late 1980s and 1990s [3][4], and even an early review article [5] exists. Compared to early work, modern methods differ markedly in their scale, neural architectures, and encoding schemes.

Current research in neural compression is heavily inspired by the advent of deep generative models, such as GANs, VAEs, normalizing flows, and autoregressive models [6], [7], [8], [9]. While these models allow us to capture complex data distributions from samples (a key to neural compression), the research tends to focus on generating realistic data [10] or achieving high data log-density [8], objectives not always aligned with data compression.

Arguably the first work exploring deep generative models for data compression appeared in 2016 [11], and the topic of neural compression has grown considerably since then. Multiple researchers have identified connections between variational inference and lossless [12][67] as well as lossy [13][14] [15][16] compression. This article hopes to further facilitate such exchange between these fields, raising awareness of compression as a fruitful application for generative modeling as well as the associated interesting challenges.

Instead of surveying the vast literature, we aim to cover the essential concepts and methods in neural compression, with a reader in mind who is versed in machine learning but
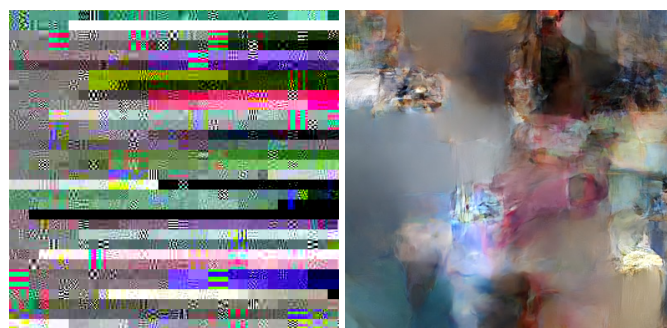
• *Yibo Yang and Stephan Mandt are with the Department of Computer Science, University of California Irvine. Lucas Theis is with Google.*

Fig. 1. Compression as generative modeling. *Left:* A sample drawn from the probabilistic model underlying JPEG, which betrays an assumption of independence among neighboring 8 by 8 pixel blocks (except for the DC components within each row). *Right:* A sample generated by a recent neural compression model by Minnen et al. [20].

not necessarily data compression. We hope to complement existing surveys that have a more applied focus on data compression [17][18][19] by highlighting the connections to generative modeling and machine learning in general.

Neural compression offers the potential for automatically constructing compression algorithms from raw data. This can be especially useful for new or domain-specific data types, such as VR content or scientific data, where developing custom codecs could otherwise be expensive. However, much of this potential remains unexplored, so we center our discussions around image compression, where most learned compression methods were first developed. Nonetheless, these methods apply more broadly to other types of data. We treat an example of sequential data, video compression, in Section 3.7. Effectively compressing such data requires more elaborate models, but the basic idea of regulating the entropy/bit-rate of learned representations and the associated techniques remain the same.

JPEG [21] serves as a good motivating example of the lossy compression pipeline (depicted in Fig. 2). First introduced in 1992, it is still one of the most widely used image compression standards [22]. At the heart of JPEG are linear mappings which losslessly transform pixels into coefficients and back. The coefficients are first quantized to integers, incurring some information loss. Then they are further com-

pressed losslessly by a combination of run-length encoding and entropy coding (the latter is discussed in Section 2.1.1).

The linear portion of the encoding process consists of several steps. First, each pixel is transformed from RGB to YCC coefficients consisting of a luma component (Y) and two color components (C). After this color transform, each channel is treated independently, and optional downsampling is applied to the color channels. Next, each channel is divided into 8×8 pixel blocks, and each block independently undergoes a *discrete cosine transform* (DCT). The transform coefficients are then linearly scaled, and rounded to integers. Given an image $\mathbf{x}$, the encoder thus performs

$$\hat{\mathbf{z}} = \lfloor \mathbf{DACx} \rceil, \tag{1}$$

where $\mathbf{C}$ is the pixelwise color transform, $\mathbf{A}$ is the block- and channelwise DCT, and $\mathbf{D}$ is a diagonal matrix scaling the coefficients. The decoder applies the transforms in reverse,

$$\hat{\mathbf{x}} = \mathbf{C}^{-1}\mathbf{A}^{\top}\mathbf{D}^{-1}\hat{\mathbf{z}}. \tag{2}$$

Readers familiar with machine learning will be reminded of autoencoders [23][24], and it is natural to consider learned neural networks in place of the linear transforms. As we will see later, there are indeed close connections between lossy compression and variational autoencoders (VAEs) [7][25], though other generative models have a role to play as well. What we call "coefficients" in the context of compression are often called "latent variables" in the context of generative models. Like generative models, JPEG defines a probability distribution over coefficients which represents assumptions about the latent representation. Just as in VAEs, we can use this distribution to draw samples from the model underlying JPEG, with an example shown in Figure 1.

Overview. This introduction is organized by two main parts, lossless (Section 2) and lossy (Section 3) compression; the latter relies on the former for compressing latent representations of the data (see Fig. 2). We begin by reviewing basic *coding theory* (Sec. 2.1), which allows us to turn the problem of lossless compression into learning a discrete data distribution. In practice, we need to decompose the potentially high-dimensional data distribution using tools from generative modeling, including *autoregressive* (Sec. 2.2), *latent-variable*, (Sec. 2.3), among *other models* (Sec. 2.4). Each model differs in its compatibility with different entropy-codes, and offers a different trade-off between the compression bit-rate and computation efficiency. *Lossy* compression then introduces additional desiderata, the most common being the *distortion* of reconstructions, based on which the classical theory and algorithms such as VQ and transform coding are reviewed (Sec. 3.1). We then introduce *neural methods* as a natural extension of transform coding (Sec. 3.2), discuss the techniques necessary for *end-to-end learning of quantized representations* (Sec. 3.3), as well as lossy compression schemes that attempt to *bypass quantization* (Sec. 3.4). We then explore additional desiderata, such as the *perceptual quality* of reconstructions (Sec. 3.5), and the usefulness of learned representations for *downstream tasks* (Sec. 3.6), before briefly reviewing *video compression* (Sec. 3.7). Finally, we conclude in Section 4 with the challenges and open problems in neural compression that may drive its future advances.
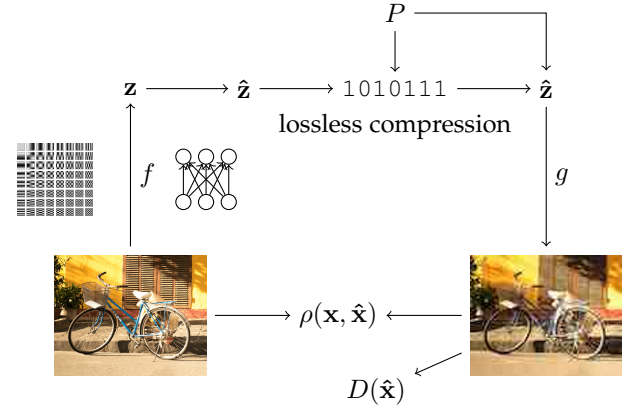

Fig. 2. A typical pipeline in both neural and classical lossy image compression. An encoder transformation f maps images to coefficients $\mathbf{z}$, which are first quantized to $\hat{\mathbf{z}}$, and then entropy encoded into bits using an entropy model P. A reconstruction $\hat{\mathbf{x}}$ is obtained using a decoder g that aims for a small distortion ρ between the data $\mathbf{x}$ and its lossy reconstruction $\hat{\mathbf{x}}$. In addition, neural compression can also involve an adversarial critic D, encouraging realism and high perceptual quality.

2 LOSSLESS COMPRESSION

Lossless compression aims to represent data with as few bits as possible such that the data can be reconstructed perfectly. The basic recipe is to first build a probabilistic model of the data, and then feed its probabilities into a so-called entropy coding scheme which converts data into compact bit-strings. This precludes non-likelihood-based models such as *generative adversarial networks* GANs [6], from which it is hard to derive probabilities and which would often assign zero probability to data even if we could evaluate them.

2.1 Background

In the first few subsections, we review the basic concepts and algorithms for *entropy coding*, which is the core interface between lossless compression and data modeling. Then in Sec. 2.1.6, we discuss a commonly used modeling technique for representing a discrete distribution with a density.

2.1.1 Entropy coding

We call a sequence of outcomes of a discrete random variable a *message*, and *entropy coding* is a way to achieve lossless compression of a message. The basic idea, as embodied by *symbol codes*, is to replace commonly occurring symbols with short codewords and rare symbols with longer codewords, thereby reducing the message's overall length. Morse code implements on this idea and represents the common letter "e" with a single so-called *dit* and the less frequent letter "s" using 3 *dits*. To be able to distinguish between the message "eee" and the message "s", Morse code additionally requires pauses between encoded letters. These extra markers can be avoided by instead using a *prefix-free* code where no codeword is the prefix of any other codeword [26].

By Shannon's source coding theorem [27], the codeword length of an optimal prefix-free code is approximately the negative logarithm of the codeword's probability. Shannon also showed that the expected message length of an optimal prefix-free code is close to the *entropy* of the message.
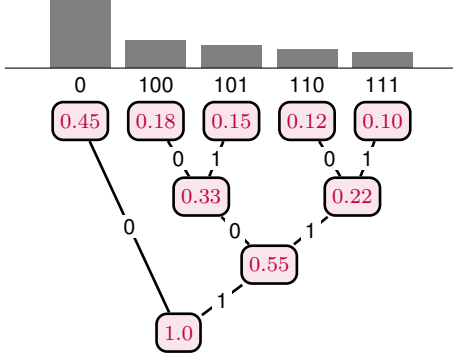
Fig. 3. Visualization of a Huffman tree over five symbols. Purple numbers in boxes denote probabilities, while binary strings above the leaf nodes correspond to the codewords assigned by the Huffman algorithm.

2.1.2 Entropy and information

The entropy[1]of a discrete random variable $\mathbf{X}$ is a measure of uncertainty about its outcomes. It is based on the concept of *surprise*, or *information content*, which can be defined as the negative log-probability of an outcome $-\log_2 P(\mathbf{x})$. Entropy, by definition, is the expected value of surprise,

$$H[\mathbf{X}] = \mathbb{E}_P[-\log_2 P(\mathbf{X})]. \tag{3}$$

For example, the entropy of a fair coin flip is 1 bit, and the entropy of a biased coin flip approaches zero bits as the probability of one of the two outcomes approaches one.

When we losslessly compress data with a prefix-code, the entropy is the minimum number of bits required on average. More precisely, the expected message length $|C(\mathbf{X})|$ of an optimal prefix-free code C is bounded as

$$H[\mathbf{X}] \leq \mathbb{E}[|C(\mathbf{X})|] \leq H[\mathbf{X}] + 1. \tag{4}$$

In practice, we typically do not know the data distribution P but need to approximate it with a distribution Q. We usually estimate Q by maximum-likelihood, or equivalently, minimizing the *cross-entropy* between P and Q, defined as,

$$H[P, Q] = \mathbb{E}_P[-\log_2 Q(\mathbf{X})]. \tag{5}$$

This is justified from a compression perspective, as the cross-entropy captures the average number of bits needed to code samples from P using a code optimized for Q. The cross-entropy is always at least as large as the entropy, and the gap between the two is called *relative entropy* or Kullback-Leibler (KL) divergence, defined as

$$D_{\mathrm{KL}}[P \parallel Q] = \mathbb{E}_P[-\log_2 Q(\mathbf{X}) + \log_2 P(\mathbf{X})]. \tag{6}$$

It is always positive unless $P = Q$ and serves as an asymmetric distance measure between the two distributions.

Based on these foundational concepts, we will review a few entropy coding schemes next.

---

1. Entropy was originally defined as a thermodynamic concept by Clausius [28] and later Boltzmann [29], while the information theoretic entropy was introduced by Shannon [27].

2.1.3 Huffman coding

Perhaps the most well-known prefix-free symbol coding approach is Huffmann coding [30]. In a nutshell, given a distribution over symbols, the algorithm assigns unique binary codewords to every symbol by building a so-called Huffman tree (Fig. 3). The leaf nodes of the tree are associated with the symbols. A Huffman tree can be recursively grown from the leaves to the root by successively merging two nodes that have the lowest probabilities. By traversing the tree from the root to a leaf, the sequence of branching directions ("0" for left, "1" for right) assigns a unique binary codeword to each symbol, with the more frequent symbols receiving shorter codewords. Encoding and decoding are simple lookup operations linear in the tree depth.

Huffman coding assigns a codeword with length at most $\lceil -\log_2 P(\mathbf{x}) \rceil$ for each symbol $\mathbf{x}$, and can be shown to be optimal among prefix codes [26]. However, as log-probabilities are generally not integers, Huffman coding (as with all so-called *symbol codes*) incurs an overhead of up to 1 bit per symbol, relative to the information content. For example, a heavily biased coin with an entropy close to 0 will still require 1 bit to encode. When compressing a sequence of symbols, *streaming codes* (see below) allow us to do so more efficiently than symbol codes by limiting the overhead to 1 bit for an entire *message* rather than each symbol.

2.1.4 Arithmetic coding

Arithmetic coding [31], also known as range coding [32], is our first example of a *streaming code*. Streaming codes differ from symbol codes in that they assign codewords to entire messages and individual symbols do not have unique codewords. Streaming codes amortize the coding cost's overhead across the whole sequence of symbols and are therefore able to get closer to the entropy.

The basic idea of arithmetic coding is to associate each symbol with a subinterval of the interval $[0, 1]$ such that the subinterval's length equals the symbol's probability. This procedure can be generalized towards encoding symbols in sequence. For two symbols, the second symbol is no longer considered a subinterval of $[0, 1]$ but a subinterval of the previous symbol's interval such that the second subinterval's length equals the two symbols' joint probability. For example, if symbol "a" has probability $1/5$ and is associated with $[0, 0.2)$, the sequence "aa" would be encoded as $[0, 0.04)$. This procedure can be iterated for sequences of arbitrary length, leading to a sequence of subintervals of decreasing size that contain each other. Any real-valued number contained in the final subinterval allows to uniquely reconstruct the sequence of symbols and therefore encodes the entire sequence. In practice, one picks a representative number which can be represented with the smallest number of bits while still being contained in the interval. By construction, the size of the final sub-interval is the product of all previous symbols' conditional probabilities, hence the probability of the sequence. Intuitively, the interval's length (i.e., the sequence's joint probability) determines the number of relevant digits of the number representing the interval, thus the code length equals the log-probability of the sequence as required for entropy codes.

Various strategies can be used to make decoding unique, e.g., by introducing an end-of-sequence symbol or specify-

ing the sequence length upfront. The advantage of arithmetic coding over Huffman coding is that the excess bits needed for encoding the message are amortized over the message length, making it more efficient. Notably, it is a first-in-first-out data structure, that is, a queue. As we will see, this makes it a convenient choice for compression with autoregressive models (Section 2.2).

2.1.5 Asymmetric numeral systems

More recent examples of streaming codes are asymmetric numeral systems (ANS) [33]. While arithmetic coding implements a queue data structure, ANS operates like a stack. In arithmetic coding, the symbol encoded first is also decoded first (first-in-first-out) while ANS decodes the last symbol first (last-in-first-out). A detailed description is beyond our scope, and we follow Bamler [34] in our summary of the main idea (see Townsend [35] for a different presentation).

Numeral systems like the decimal or binary system can be interpreted as optimal codes for uniform distributions over a finite alphabet (the "base" of the numeral system). They encode a sequence of enumerated symbols into a single integer number, the "stack". To encode a symbol, we multiply the stack with the base (e.g., 2 or 10) and add the symbol. To decode, we recover the symbol as the stack modulo its base, while we shorten the stack by dividing it by the base. The stack's length in binary representation is approximately the number of symbols times the logarithm of the base of the numeral system, consistent with entropy coding. Interestingly, the stack's base can be changed from symbol to symbol and it is still possible to recover the sequence as long as the inverted order of bases is used upon decoding.

ANS generalizes numeral systems from uniform probability distributions to non-uniform ones. Similar to arithmetic coding, symbols are first represented as subintervals of the unit interval. In addition, one discretizes the unit interval using a fine discretization grid. Every point on the grid belongs to the subinterval of a symbol and can be used to represent that symbol. The discretization points form a new alphabet of symbols that can be encoded using a numeral system, as described above. Since there are multiple discretization points in each each subinterval, naively encoding one of them leads to a redundant code. However, ANS is able to avoid this redundancy. Bamler [34] notes that the mechanism by which ANS achieves this can be interpreted as a bits-back coding procedure, which will be discussed in Section 2.3.2. Like arithmetic coding, ANS incures an overhead of up to 1 bit per message.

2.1.6 Continuous models for discrete data

In this subsection, we show how a model for discrete data can be defined and parameterized by a continuous model, a common technique in generative modeling and neural compression. Lossless compression generally operates on discrete data. After all, it is infeasible to losslessly encode any real number by a finite number of bits. However, many generative models in machine learning assume continuous data, and model it with a density function. It turns out such continuous models are still useful for lossless compression.

Suppose we have a density model q over $\mathbb{R}^D$, and $\mathbf{x} \in \{0, \ldots, 255\}^D$ is an RGB image following the ground truth image distribution P. We can derive a PMF over integers by integrating the density over hypercubes, as follows,

$$Q(\mathbf{x}) := \int_{[-.5,.5)^D} q(\mathbf{x} + \mathbf{u}) \, d\mathbf{u}. \tag{7}$$

Now we add uniform noise $\mathbf{u} \in [-0.5, 0.5)^D$ to the data, so that the noisy data, $\mathbf{y} = \mathbf{x} + \mathbf{u}$, has an induced density p. Then it is not difficult to show that [36]

$$-\int p(\mathbf{y}) \log_2 q(\mathbf{y}) \, d\mathbf{y} \geq -\sum_{\mathbf{x}} P(\mathbf{x}) \log_2 Q(\mathbf{x}), \tag{8}$$

i.e., we can minimize an upper bound on the lossless compression cost under the discretized model (RHS) by fitting a density via maximum likelihood (LHS), provided the discrete data is *dequantized* appropriately with noise [37].

The form of Q as defined in Eq. 7, which we call a *discretized density model*, is also useful in itself as a flexible model for discrete data. Examples include PixelCNN++ [38], the prior distribution in a discrete flow [39], as well as entropy models for neural compression [40][41][42].

The integral in Eq. 7 in general is intractable to compute, but it can often be broken down into a series of univariate integrals for the models we discuss. Therefore let us consider a univariate version of the discretized density model,

$$Q_\theta(x) := \int_{[-0.5, 0.5)} q_\theta(x + u) du.$$

Let F_θ denote the CDF of q_θ, we can equivalently express the above in terms of a difference of CDF evaluations:

$$Q_\theta(x) := F_\theta(x + 0.5) - F_\theta(x - 0.5). \tag{9}$$

e.g., if q_θ is the density of a logistic distribution, then F_θ is the logistic sigmoid function common in deep learning.

2.2 Autoregressive models

Autoregressive models exploit the fact that we can write any probability distribution as a product of conditional distributions using the chain rule of probabilities [43],

$$p(\mathbf{x}) = \prod_i p(x_i \mid \mathbf{x}_{<i}). \tag{10}$$

Here, x_i is the i-th entry of the vector $\mathbf{x}$ and $\mathbf{x}_{<i}$ corresponds to all previous entries in an arbitrary order. The autoregressive factorization does not make any assumptions about the data distribution yet still allows us to easily incorporate useful assumptions. For example, a Markov assumption can be implemented by only considering the entries in $\mathbf{x}_{<i}$ which are close to i. A stationarity assumption is easily incorporated by using the same conditional distribution $p(x_i \mid \mathbf{x}_{<i})$ at every location. These two assumptions are often reasonable and can drastically reduce the amount of parameters of a model.

Autoregressive modeling lends itself to lossless compression in combination with arithmetic coding (Section 2.1.4) since both deal with data sequentially, one symbol at a time. Each symbol is encoded using the conditional distribution given the data that has already been encoded. This is in contrast to Markov random fields, for example, where conditional distributions are typically only tractable when conditioning on a larger neighborhood. Entropy coding generally requires the number of symbols in each

encoding step to be manageable. Autoregressive models provide an important step towards practical entropy coding by decomposing a high-dimensional distribution into low-dimensional conditional distributions. Arithmetic coding is a better match for autoregressive models than ANS since it operates like a queue. Symbols encoded earlier will also be decoded earlier and therefore will be available as input to conditional distributions.

For data modalities such as audio or text, autoregressive models are an obvious choice due to the signal's sequential nature. Indeed, two of the top performing algorithms in the Large Text Compression Benchmark [44] use recurrent neural networks to predict the next token of a sentence. While `cmix` [45] uses a mixture of long short-term memory networks (LSTMs) [46] and nonparametric models, `nncp` [47] relies solely on neural network models. However, autoregressive models have long also found application in image compression. For example, JPEG [21] encodes the difference between neighboring DC coefficients, $z_{ij}^{\mathrm{DC}} - z_{i(j-1)}^{\mathrm{DC}}$, in a raster-scan order, which can be thought of as implementing a first-order Markov model.

Mixtures of experts [48][49][50] are a class of autoregressive models proven useful for compressing images,

$$p(x_{ij} \mid \mathbf{x}_{<ij}) = \sum_k \underbrace{p(k \mid \mathbf{x}_{<ij})}_{\text{Gates}} \underbrace{p(x_{ij} \mid \mathbf{x}_{<ij}, k)}_{\text{Experts}}. \quad (11)$$

The basic idea behind neural network extensions of this approach is to nonlinearly transform the inputs $\mathbf{x}_{<ij}$ before feeding them into the gates and the experts. For instance, RNADE [37] used a fully connected neural network with a single rectified linear layer to transform the inputs $\mathbf{x}_{<ij}$. Other examples of deep autoregressive models include RIDE [51], PixelRNN [52], or PixelCNN++ [38]. More recent autoregressive modeling papers continue to explore different architectures for transforming $\mathbf{x}_{>ij}$. For example, the Image Transformer [53] uses an architecture based on self-attention [54]. PixelSNAIL [55] uses a combination of convolutions and self-attention layers. Glow [56] uses invertible flows.

With the exception of `nncp` [47] and `cmix` [45], all autoregressive models mentioned so far are *static* models. That is, the models' parameters are trained once and then remain fixed during the entire encoding and decoding process. In contrast, a *dynamic* model updates its parameters during the encoding process based on already encoded data. The decoder is then able to apply the same model updates based on the data already received. A simple dynamic autoregressive model for images was proposed by Wu et al. [57]. Here, the predictors are linear but the predictor's parameters are chosen dynamically. This is done by treating a larger neighborhood of preceding pixels as training data for the predictor. Meyer and Tischer [58] improved on this idea by weighting training points based on their distance to the pixel whose value we are predicting.

Autoregressive models come with the restriction that decoding is an inherently sequential procedure. Each symbol can only be decoded after all the symbols have been decoded on which its prediction depends. To improve decoding speed, we can restrict the context $\mathbf{x}_{<i}$ to only a small neighborhood around $\mathbf{x}_i$, as for example in JPEG.

Furthermore, the degree of parallelism can be increased by grouping coordinates of the data into blocks and only modeling the conditional dependencies between blocks, while treating data coordinates within each block as conditionally independent [59].

2.3 Latent variable models

Latent variable models represent the data distribution using the sum rule of probability,

$$p(\mathbf{x}) = \int p(\mathbf{x}, \mathbf{z}) \, \mathrm{d}\mathbf{z} = \int p(\mathbf{x} \mid \mathbf{z}) p(\mathbf{z}) \, \mathrm{d}\mathbf{z}, \quad (12)$$

where $\mathbf{z}$ is a vector of *latent variables* (also called "latents"), and the joint distribution $p(\mathbf{x}, \mathbf{z})$ factorizes into a *prior* $p(\mathbf{z})$ and a *likelihood* $p(\mathbf{x} \mid \mathbf{z})$. Latent variable models are ubiquitous in machine learning and include hidden Markov models, mixture models [43], and more recently variational autoencoders (VAEs) [7][25]. By integrating or summing over all possible realizations of the latent vector, latent variable models can capture complex dependencies in the data even when the prior and likelihood take simple forms.

Training a latent variable model by (approximate) maximum-likelihood (see Eq. 5) comes with a main challenge: unlike in a fully-observed (e.g., autoregressive) model where the data probability $p(\mathbf{x})$ can be readily evaluated, doing so is no longer straightforward since it is defined through an often intractable integral (Eq. 12). Variational inference deals with exactly these complications, and we refer to Zhang et al. [60] for more details on these methods. Here, we instead focus on the compression problem, which faces a similar challenge and uses similar tools. Given a latent variable model consisting of a prior $p(\mathbf{z})$ and likelihood $p(\mathbf{x}|\mathbf{z})$, our goal is to compress a given data vector $\mathbf{x}$ with a code length close to its information content under the model, $-\log_2 p(\mathbf{x})$. To simplify the discussion below, we assume discrete $\mathbf{z}$ unless specified otherwise.

2.3.1 Two-part code

We start by considering a simple although generally suboptimal *two-part code* [61]. Here, the data $\mathbf{x}$ is transmitted along with a latent vector $\mathbf{z}$ in two steps. First, the sender decides on a (ideally informative) vector $\mathbf{z}$, encodes and transmits it under the prior $p(\mathbf{z})$. Next, $\mathbf{x}$ is compressed and transmitted under the likelihood model, $p(\mathbf{x} \mid \mathbf{z})$. The receiver then decodes $\mathbf{z}$, and finally $\mathbf{x}$ given $\mathbf{z}$, using the same models. Both the prior and likelihood models are often fully factorized, allowing for coding each dimension of $\mathbf{z}$ or $\mathbf{x}$ in parallel, but can also be autoregressive models used in conjunction with arithmetic coding. Assuming negligible entropy coding overhead, the combined code length is

$$l(\mathbf{x}, \mathbf{z}) = -\log_2 p(\mathbf{z}) - \log_2 p(\mathbf{x}|\mathbf{z}) = -\log_2 p(\mathbf{x}, \mathbf{z}). \quad (13)$$

Moreover, the sender can (at least in principle) minimize this quantity over all choices of $\mathbf{z}$, resulting in the code length

$$l_{\mathrm{MTP}}(\mathbf{x}) = \min_{\mathbf{z}} \left(-\log_2 p(\mathbf{z}) - \log_2 p(\mathbf{x} \mid \mathbf{z}) \right). \quad (14)$$

The minimal two-part code length, $l_{\mathrm{MTP}}(\mathbf{x})$, is generally still suboptimal[2] [12][62][63]. To see this, consider the following bound on the information content $-\log_2 p(\mathbf{x})$,

$$-\log_2 p(\mathbf{x}) \leq -\log_2 p(\mathbf{x}) + D_{\mathrm{KL}}[q(\mathbf{z} \mid \mathbf{x}) \parallel p(\mathbf{z} \mid \mathbf{x})] \quad (15)$$

$$= \mathbb{E}_{q(\mathbf{z}|\mathbf{x})}[-\log_2 p(\mathbf{z}, \mathbf{x})] - \mathbb{H}[q(\mathbf{z} \mid \mathbf{x})], \quad (16)$$

also known as the *negative evidence lower bound* (NELBO) of variational inference [60]. Here, q is any distribution over $\mathbf{z}$ which may depend on $\mathbf{x}$. Crucially, the minimal two-part code length (Eq. 14) is a special case of the NELBO where

$$q(\mathbf{z} \mid \mathbf{x}) = \delta_{\mathbf{z}_{\min}}(\mathbf{z}) \quad (17)$$

is a degenerate distribution centered on $\mathbf{z}_{\min}$, which achieves the minimum in Eq. 14. In this case the entropy term vanishes. More generally, the NELBO is minimized when $q(\mathbf{z} \mid \mathbf{x})$ equals the Bayesian *posterior* distribution $p(\mathbf{z} \mid \mathbf{x})$, the target of approximate inference [60].

One may naturally wonder whether a coding cost equal to the NELBO can be realized for *any choice of* $q(\mathbf{z} \mid \mathbf{x})$. Bits-back coding, to be discussed next, answers this question in the affirmative. It further offers a compression interpretation of variational inference: for a given latent variable model, reducing the KL divergence between the distribution q and the posterior distribution is equivalent to minimizing the code length of $\mathbf{x}$ under bits-back coding.

2.3.2 Bits-back coding

While the optimal two-part code chooses a best latent vector $\mathbf{z}$ using deterministic optimization, bits-back coding [64][62][65][63] instead uses a *stochastic* latent code in the form of a sample $\mathbf{z}$ from a distribution q. Surprisingly, this stochastic code can save bits compared to a deterministic code by allowing auxiliary information to piggyback on the choice of the latent code. To gain some intuition, consider again the optimization in Eq. 14 for picking the optimal two-part code. When the given data $\mathbf{x}$ is uninformative of what latent variable $\mathbf{z}$ generated it, the minimization over $\mathbf{z}$ may find multiple candidates that are nearly optimal. In the extreme case, ties need to be broken to settle on one of many equally good candidates. Instead of choosing a $\mathbf{z}_i$ randomly, the encoder can do so intentionally so as to communicate additional information via the chosen index i, provided that the decoder can reverse-engineer the encoding procedure.

Before proceeding, we emphasize a connection between sampling and decoding random bits. Given an entropy code derived from a discrete distribution, using it to *decode* a sequence of uniformly random bits produces a random sample from this distribution. For example, consider decoding a random bit string according to a Huffman tree (Fig. 3). As we traverse from the root to any leaf node, every edge along the path corresponds to a decision according to a coin flip. The probability of ending up with a particular symbol $\mathbf{x}$ with code length $|C(\mathbf{x})|$ is $2^{-|C(\mathbf{x})|}$, or approximately $2^{\log_2 p(\mathbf{x})} = p(\mathbf{x})$.

In bits-back coding, the sender first generates a sample $\mathbf{z} \sim q(\mathbf{z} \mid \mathbf{x})$ by *decoding* a random bit string ξ. Next, the

---

2. However, it is possible to directly optimize a neural compression method for the two-part code. e.g., Mentzer et al. [40] trained a latent variable model with an inference network to minimize the expected coding cost of the two-part code, demonstrating much faster decoding speed than autoregressive models, although at $\sim 20\%$ worse bit-rate.
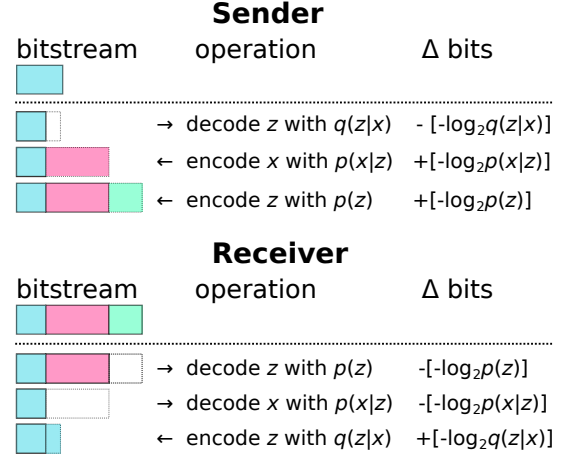

Sender

bitstream	operation	Δ bits
	$\rightarrow$ decode z with $q(z\|x)$	- [-$\log_2 q(z\|x)$]
	$\leftarrow$ encode x with $p(x\|z)$	+[-$\log_2 p(x\|z)$]
	$\leftarrow$ encode z with $p(z)$	+[-$\log_2 p(z)$]

Receiver

bitstream	operation	Δ bits
	$\rightarrow$ decode z with $p(z)$	-[-$\log_2 p(z)$]
	$\rightarrow$ decode x with $p(x\|z)$	-[-$\log_2 p(x\|z)$]
	$\leftarrow$ encode z with $q(z\|x)$	+[-$\log_2 q(z\|x)$]

Fig. 4. An illustration of the encoding (sender) and decoding (receiver) operations of bits-back coding. Auxiliary bits (ξ) are colored in blue.

sender encodes $\mathbf{x}$ under $p(\mathbf{x} \mid \mathbf{z})$, then $\mathbf{z}$ under $p(\mathbf{z})$, and then transmits the resulting bits. The receiver begins by decoding $\mathbf{z}$ and $\mathbf{x}$ from the received bits just as in the two-part code, but then proceeds to recover the exact bit string the sender used to generate $\mathbf{z}$. This can be done by *encoding* $\mathbf{z}$ under the distribution $q(\mathbf{z} \mid \mathbf{x})$, which we assume the receiver has access to. Thus, $-\log_2 q(\mathbf{z}|\mathbf{x})$ bits worth of information are automatically recovered after decoding $\mathbf{x}$ and $\mathbf{z}$, giving the scheme its name "bits-back". Finally, and crucially, we note that the initial bits used to generate $\mathbf{z}$ do not have to be truly random. Indeed, to be useful they should be supplied from a stream of already compressed data or some useful *auxiliary information*. This could be, or example, the bitstring of a small thumbnail image encoded with JPEG.

Fig. 4 graphically summarizes the algorithm. Given a bitstring ξ of auxiliary bits and the data $\mathbf{x}$ to transmit, the sender starts by decoding a portion of ξ into a stochastic latent code $\mathbf{z}$ of the data, ultimately sending a total number of bits equal to $|\xi| - \log_2 p(\mathbf{z}) - \log_2 p(\mathbf{x}|\mathbf{z}) + \log_2 q(\mathbf{z}|\mathbf{x})$ to communicate both ξ and $\mathbf{x}$. The net number of bits used for transmitting $\mathbf{x}$ alone is therefore

$$-\log_2 p(\mathbf{z}) - \log_2 p(\mathbf{x}|\mathbf{z}) - (-\log_2 q(\mathbf{z}|\mathbf{x})) \quad (18)$$

which corresponds to a discount of $-\log_2 q(\mathbf{z} \mid \mathbf{x})$ bits compared to a two-part code. Since $\mathbf{z}$ was drawn from $q(\mathbf{z}|\mathbf{x})$, the expected coding cost is exactly the NELBO [60].

As we saw, the sender must be committed to transmit at least $-\log_2 q(\mathbf{z} \mid \mathbf{x})$ many auxiliary bits; otherwise the proper bits-back discount cannot be obtained, resulting in a worse coding cost. To get around this *initial bits problem*, bits-back coding is often used to jointly compress a sequence of data points $\mathbf{x}_1, ..., \mathbf{x}_n$. The idea, referred to as *chaining* [66] or "bits-back with feedback" [12], is that the bit string of previously encoded data points $\mathbf{x}_1, ..., \mathbf{x}_{i-1}$ provides a natural source of auxiliary bits for encoding the next data point $\mathbf{x}_i$. Chaining poses a requirement on the entropy coder that data is decoded in the exact opposite order in which it is encoded. Bits-back is therefore naturally combined with ANS coding which operates in stack order (Section 2.1.1), popularized by the BB-ANS algorithm [66].

2.3.3 Improvements and extensions

Continuous latents. When the latent vector is continuous, bits-back coding can still be applied after discretizing the latent space and associated distributions [67][66]. More finely discretized latents will require more bits to encode, exacerbating the initial bits problem, but allow us to recover an equal amount of bits back. Bits-back coding thus allows us to code continuous latents with arbitrarily high precision.

Extension to models with multiple latents. Although our discussion focused on a model with a single latent tensor, Ho et al. [68] and Townsend et al. [69] extended bits-back coding to hierarchical latent variable models, leveraging their superior expressiveness (in terms of better NELBO) to improve compression performance. Bit-Swap [68], in particular, places restrictions on the latent hierarchy (e.g., Markovian) to allow recursive bits-back coding, alleviating the initial-bits problem. Ruan et al. [70] and Townsend et al. [71] developed bits-back schemes for sequential (e.g., time-series) latent variable models.

Iterative inference. As discussed in Sec. 2.3.1, the over-head of bits-back coding is equal to the KL divergence between $q(\mathbf{z} \mid \mathbf{x})$ and the true posterior $p(\mathbf{z} \mid \mathbf{x})$. The parameters of q (e.g., mean of a Gaussian) are typically predicted from $\mathbf{x}$ by an *amortized inference* network, as in a VAE (see, e.g., [7]). Although cheap to compute, the resulting q distribution is generally suboptimal [72]. Yang et al. [16] took a pre-trained model [42] and proposed to directly minimize the KL gap with respect to the q parameters for each given data point $\mathbf{x}$, resulting in improved image compression performance.

Extended latent spaces. Analogous to the importance-weighted ELBO [73], importance-weighted NELBO provides a tighter variational upper bound on the ideal code length than the NELBO (Eq. 16). Ruan et al. [70] and Theis et al. [74] proposed bits-back coding schemes that operate in an extended latent space and operationalize the coding cost of the importance-weighted NELBO, and demonstrated improved compression performance.

2.4 Invertible flows and other models

Normalizing Flows. Although *continuous* normalizing flows do not lend themselves directly to lossless compression, local bits-back coding [68] allows lossless compression of finely quantized continuous data, with a code length close to the negative log data density up to a constant dependent on the quantization precision. The same method also allows losslessly compressing discrete data using a flow trained on the dequantization objective (e.g., the LHS of Eq. 8). By contrast, *discrete normalizing flows* [39][75] directly model integer-valued data and support lossless compression. Such a flow learns a bijection f to map data to an integer latent space, where a factorized prior is assumed; the given data $\mathbf{x}$ can then be compressed by simply entropy-coding its latent representation $f(\mathbf{x})$, and decompressed using f^{-1}. This can be viewed as bits-back coding with a deterministic q.

Other Models. New types of generative models continue to be explored for lossless compression, aiming to achieve greater modeling power (hence better compression rate), while reducing computational demands. Promising recent examples include probabilistic circuits [76], which offer fast

encoding/decoding time and lightweight models, and discrete diffusion models [77][78], which offer parallel encoding/decoding and improved single-image compression rate.

3 LOSSY COMPRESSION

In the following we review neural *lossy* compression, that is, compression with imperfect data reconstruction. After a brief introduction, we discuss basic theoretical background (Section 3.1), neural lossy compression (Section 3.2), perceptual losses (Section 3.5), compression without quanization (Section 3.4), and video compression (Section 3.7).

Frequently, we make reference to the *quantization* operation, denoted by $[\![\cdot]\!]$. Quantization can be implemented in various ways in neural compression (e.g., by rounding to the nearest integer, denoted by $\lfloor\cdot\rceil$; we give a detailed treatment in Section 3.3), but at a high level is understood to be any mapping, either deterministic or stochastic, from a (usually continuous) set of input to a *countable* set of output values.

3.1 Background

The main feature distinguishing lossy compression from lossless compression is that the decoder obtains an imperfect, or *distorted*, reconstruction of the original data. This extra flexibility allows for more effective compression. For example, lossy reconstruction is sufficient and widely used for transmitting digital media such as images and videos. For continuous data, which cannot be perfectly represented by a finite bitstring, lossy compression is also a practical necessity. We give an overview of the classical theory of lossy compression, the closely related vector quantizer, and its computationally improved version — transform coding, which is arguably the precursor to neural lossy compression.

3.1.1 Rate-distortion theory

We consider a lossy compression algorithm (or a lossy *codec*) to be a 3-tuple consisting of an encoder, decoder, and an entropy code, denoted by $c = (\mathtt{e}, \mathtt{d}, \gamma)$. The *encoder* $\mathtt{e} : \mathcal{X} \to \mathcal{S}$ maps each data point $\mathbf{x}$ to an element of a discrete set $\mathcal{S}$ (e.g., a subset of natural numbers). The *decoder* $\mathtt{d} : \mathcal{S} \to \hat{\mathcal{X}}$ maps each encoding s to a *reconstruction point* $\hat{\mathbf{x}} \in \hat{\mathcal{X}}$.

The encoder and decoder further agree to transmit the symbols of $\mathcal{S}$ under an *entropy code* γ (see Sec.2.1.1); we write $l(\mathbf{x}) := |\gamma(\mathtt{e}(\mathbf{x}))|$ to denote the code length assigned to the encoding of $\mathbf{x}$. Suppose we are given a *distortion function* $\rho : \mathcal{X} \times \hat{\mathcal{X}} \to [0, \infty)$ that measures the error caused by representing $\mathbf{x}$ with the lossy reconstruction $\hat{\mathbf{x}}$ (e.g., squared error $\|\mathbf{x} - \hat{\mathbf{x}}\|^2$). Lossy compression is then generally concerned with minimizing the average *distortion*

$$\mathcal{D} = \mathbb{E}[\rho(\mathbf{x}, \hat{\mathbf{x}})] = \int \rho(\mathbf{x}, \hat{\mathbf{x}}) p_{data}(\mathbf{x}) \mathrm{d}\mathbf{x}, \qquad (19)$$

and simultaneously, the *rate*

$$\mathcal{R} = \mathbb{E}[l(\mathbf{x})] = \int l(\mathbf{x}) p_{data}(\mathbf{x}) \mathrm{d}\mathbf{x}, \qquad (20)$$

that is, the average number of bits needed to encode the data. We want to minimize these two quantities with respect to the choice of the encoding and decoding procedures $\mathtt{e}$ and $\mathtt{d}$, as well as the entropy code γ.

Rate-distortion (R-D) theory [79] [26] establishes limits on the performance of any such algorithm. Any lossy compression algorithm implements a noisy channel that receives a data input $\mathbf{x}$ and outputs a reconstruction $\hat{\mathbf{x}}$, described by a conditional distribution $p(\hat{\mathbf{x}} \mid \mathbf{x})$. The mutual information $I[\mathbf{x}, \hat{\mathbf{x}}]$ expresses the information transmitted, and for a given distortion threshold D, the lowest achievable rate is characterized by the information *rate-distortion function* [79],

$$\mathcal{R}_I(D) = \inf_{p(\hat{\mathbf{x}}|\mathbf{x}):\mathbb{E}[\rho(\mathbf{x},\hat{\mathbf{x}})]\leq D} I[\mathbf{x}, \hat{\mathbf{x}}], \qquad (21)$$

where $\mathbb{E}[\rho(\mathbf{x}, \hat{\mathbf{x}})]$ and $I[\mathbf{x}, \hat{\mathbf{x}}]$ are defined with respect to the joint distribution $p_{data}(\mathbf{x})p(\hat{\mathbf{x}}|\mathbf{x})$. The (information) R-D function is thus a fundamental quantity that generalizes the Shannon entropy H (Eq. 3) from lossless compression to lossy compression, but is generally unknown analytically. It can be estimated by the Blahut-Arimoto algorithm [26] when the data and reconstruction spaces are discrete and low-dimensional, and recently Yang and Mandt [80] proposed a machine learning approach for estimating the rate-distortion function in a significantly more general setting.

In theory, the optimal rate $\mathcal{R}_I(D)$ is achievable by vector quantization [26], described next (Section 3.1.2), but this approach to compression quickly becomes intractable for high-dimensional data. Rather than trying to achieve the theoretically optimal rate $\mathcal{R}_I(D)$ with any codec at any computational cost, in practice the design of a lossy codec is constrained by practical considerations, such as the computation budget of the target hardware, or the decoding latency acceptable for the application. Denoting the set of all the acceptable codecs under consideration by $\mathcal{C}$, we can instead consider an *operational* rate-distortion tradeoff, formalized by

$$\mathcal{R}_O(D) = \inf_{c\in\mathcal{C}:\mathbb{E}[\rho(\mathbf{x},\hat{\mathbf{x}})]\leq D} \mathbb{E}[l(\mathbf{x})]. \qquad (22)$$

Compared to Eq. 21, we replaced mutual information by the operational rate and optimize over an actual lossy codec c. We can relax the constrained optimization problem to an uncontrained one, by introducing the Lagrangian [81],

$$L(\lambda, c) = \mathcal{R}(c) + \lambda\mathcal{D}(c) = \mathbb{E}[l(\mathbf{x})] + \lambda\mathbb{E}[\rho(\mathbf{x}, \hat{\mathbf{x}})]. \quad (23)$$

For each fixed $\lambda > 0$, minimizing the above rate-distortion Lagrangian yields a codec c^* whose operational distortion-rate performance, $(\mathcal{D}(c^*), \mathcal{R}(c^*))$, lies on the convex hull of the operational R-D curve (see Fig. 5). Codecs with different operational rate-distortion trade-offs can be found by minimizing the Lagrangian with various λ. Most current end-to-end learned lossy compression methods to be discussed in Section 3.2 follow this approach, training one codec for each λ. We note that theoretically, it is not always possible to attain every point on the operational R-D curve with this approach [82], and alternative approaches exist [83], [84].

3.1.2   *Vector Quantization*

Vector quantization (VQ), a classical technique from signal processing, is perhaps the most basic form of a lossy codec. A quantization scheme in VQ consists of a set $\hat{\mathcal{X}}$ of quantization points (usually a subset of the data space $\mathcal{X}$), and an assignment rule $\mathbf{x} \to \hat{\mathbf{x}}$, which corresponds precisely to the composition $\mathtt{d} \circ \mathtt{e}$ in the notation of Sec. 3.1.1. The goal
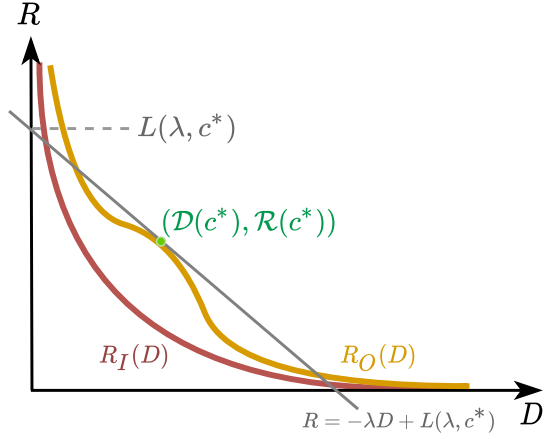

Fig. 5. Visualizing the operational R-D optimization problem. We adjust our codec c to minimize the R-axis intercept of a straight line (gray) with slope $-\lambda$ and passing through $(\mathcal{D}(c), \mathcal{R}(c))$; an optimum occurs when the line becomes tangent to the operational R-D curve R_O at the point $(\mathcal{D}(c^*), \mathcal{R}(c^*))$. Note that the operational R-D curve (orange) lies above the information R-D curve R_I (red), and is not necessarily convex.

is then to determine an optimal quantization scheme for a given data distribution, under some objective. Commonly, the objective is to minimize a reconstruction error (Eq. 19), as in the k-means algorithm, but can also more generally be an operational rate-distortion trade-off (Eq. 22).

For some data source, e.g., the uniform or the Laplace distribution, optimal quantization can be characterized analytically [85][86]. In most applications, Loyd-Max-style algorithms [87][81] (including k-means) are used instead to estimate a quantization scheme from data samples. This usually involves minimizing an empirical rate-distortion cost (Eq. 23) over a dataset, which is still a basic ingredient in today's learned compression approaches [17] (see Sec. 3.2).

Given unlimited data and compute, VQ can approximate any data distribution arbitrarily well – in fact, the theoretical limit of lossy compression, the information rate-distortion function $\mathcal{R}_I(D)$, can be shown to be achieved by jointly quantizing multiple data samples together with increasingly long blocks [26]. However, VQ comes with the severe downside of poor scalability and data efficiency [88]. The computational and storage demand of VQ increases quickly with the data dimensionality. Moreover, in high dimensions, an exceedingly large number of quantization points and high amounts of training data are needed to approximate the data distribution well. As a result, VQ is typically found in low-rate/high-distortion applications, such as low-rate speech coding [89].

3.1.3   *Transform coding*

Instead of quantizing the data in its original representation, it is often much easier to do so in a transformed space, where the representation of the data is uncorrelated. The core idea behind transform coding [90] is therefore to divide the task of lossy compression into decorrelation and quantization: first, the sender applies an *analysis transform* f to data $\mathbf{x}$, resulting in a vector $\mathbf{z} = f(\mathbf{x})$ which ideally follows a factorized distribution; and second, coordinate-wise scalar quantization $\llbracket \cdot \rrbracket$ is applied to obtain a discretized representation $\hat{\mathbf{z}} = \llbracket \mathbf{z} \rrbracket$. The symbols representing $\hat{\mathbf{z}}$ can then be converted

to a bitstring by entropy coding under an entropy model $P(\hat{\mathbf{z}})$. The receiver, upon receiving the bitstring, decodes it to recover $\hat{\mathbf{z}}$, and computes a reconstruction $\hat{\mathbf{x}} = g(\hat{\mathbf{z}})$ using a *synthesis transform* g. In the terminology of Section 3.1.1, the encoder $\mathbf{e} = [\![\cdot]\!] \circ f$ is the composition of the analysis transform f followed by quantization, and the decoder $\mathbf{d}$ is implemented by the synthesis transform g.

Unlike vector quantization, which effectively optimizes over all possible choices of encoder $\mathbf{e} : \mathcal{X} \to \mathcal{S}$ and decoder $\mathbf{d} : \mathcal{S} \to \hat{\mathcal{X}}$, transform coding implicitly restricts the solution space of allowable codecs, e.g., the set of quantization points must be in the range of g, and therefore generally cannot achieve the unconstrained optimal performance of VQ. The lack of theoretical optimality of transform coding is more than made up for by its vastly superior scalability over VQ, as evidenced by its wide-spread use in the compression of digital media, such as images and videos [90].

3.2 Neural lossy compression

Most current neural lossy compression methods are based on the paradigm of *nonlinear transform coding* [17] and use learned functions to encode data into a discrete representation, typically by quantizing a continuous representation. As follows, we review basic concepts and architectures, deferring a full discussion on model training to Section 3.3.

3.2.1 Overview

Building on transform coding (Section 3.1.3), a neural compression algorithm implements the analysis transform f and synthesis transform g using neural networks. The transformed representation $\mathbf{z} = f(\mathbf{x})$ is often referred to as a latent representation, or simply "latents", due to the connection to latent variable modeling. As in transform coding, we need a probability model P of the discretized representation $\hat{\mathbf{z}} = [\![\mathbf{z}]\!]$, called an *entropy model*, in order to entropy code $\hat{\mathbf{z}}$ into a short bit string and back (Section 2.1.1). The entropy models are often based on powerful models from neural lossless compression (Section 2). Most commonly, the objective is to simultaneously minimize the rate,

$$\mathcal{R} := \mathbb{E}[-\log_2 P([\![f(\mathbf{x})]\!])], \qquad (24)$$

and the distortion,

$$\mathcal{D} := \mathbb{E}[\rho(\mathbf{x}, g([\![f(\mathbf{x})]\!]))].$$

The expectations are taken w.r.t. the data distribution p_{data} and are estimated with data samples. Unlike in Section 3.1.1, here we no longer concern ourselves with an entropy code γ. Instead, we directly optimize with the information content in place of a code length in Eq. 24, knowing that an entropy code can (in principle) always be derived from P such that $-\log_2 P(\cdot) \approx |\gamma(\cdot)|$ (see Section 2.1.1). If we denote the true marginal distribution of $\hat{\mathbf{z}}$ by $P^*(\hat{\mathbf{z}})$ (which is induced by p_{data} and the encoding procedure in a complex way), then the rate loss can be equivalently written as the cross entropy,

$$\mathcal{R} = \mathbb{E}_{P^*(\hat{\mathbf{z}})}[-\log_2 P(\hat{\mathbf{z}})], \qquad (25)$$

which precisely captures the cost of entropy coding $\hat{\mathbf{z}} \sim P^*(\hat{\mathbf{z}})$ under our model $P(\hat{\mathbf{z}})$, and serves as an upper bound to the entropy $\mathbb{H}[P^*(\hat{\mathbf{z}})]$.

Analogous to Eq. 23, we can form a Lagrangian objective by a linear combination of rate and distortion, with $\lambda > 0$:

$$\mathbb{E}[-\log_2 P([\![f(\mathbf{x})]\!])] + \lambda \mathbb{E}[\rho(\mathbf{x}, g([\![f(\mathbf{x})]\!]))]. \qquad (26)$$

Denoting the reconstruction again by $\hat{\mathbf{x}} = g([\![f(\mathbf{x})]\!])$, the objective bears a close resemblance to that of a regularized autoencoder [23][24], where the analysis and synthesis transforms f and g correspond to the encoder [3] and decoder of an autoencoder, the distortion term $\lambda \mathbb{E}[\rho(\mathbf{x}, \hat{\mathbf{x}})]$ corresponds to a reconstruction error, and the rate term can be seen as a regularizer imposed on the representation $\hat{\mathbf{z}}$. Unlike in traditional autoencoders, where some form of compression is achieved by requiring the representation to have low dimensionality or sparsity [91], learned compression instead aims to reduce the bits-per-sample information cost of data compression, as measured by the rate term.

3.2.2 Neural Transform Architectures

Feedforward neural networks are most often used for the encoding and decoding transforms (f, g) in lossy compression, as in traditional autoencoders. For compressing unstructured data, fully-connected neural networks have been used [17], [80]. In image compression, the networks are typically convolutional neural networks (CNNs), with f implementing downsampled convolutions, and g typically implementing upsampled convolutions [92] or sub-pixel convolutions [14][93]. From the perspective of transform coding, it is not yet clear if these CNN architectures borrowed from computer vision research are most effective at decorrelating the input, and some techniques, such as Generalized Divisive Normalization [92], have been proposed to improve the transforms in this regard. We refer to [17], [94] for discussions on network capacity and its effect on computation and compression performance, but note that in the low-distortion regime, higher capacity transforms (e.g., by increasing the number of filters in a CNN) are generally needed to maximize the rate-distortion performance [13].

Recurrent architectures. Instead of encoding data $\mathbf{x}$ into $\mathbf{z}$ with a single neural network, it can be beneficial to introduce a feedback mechanism to involve the decoder in the encoding process. We may divide the compression of $\mathbf{x}$ into T stages, each stage generating an incremental representation $\hat{\mathbf{z}}_t$ from the encoder to the decoder, and the final $\hat{\mathbf{z}}$ consisting of the concatenation $\hat{\mathbf{z}}_1, \hat{\mathbf{z}}_2, ..., \hat{\mathbf{z}}_T$. At the beginning of stage t, the decoder has available a tentative data reconstruction $\hat{\mathbf{x}}_{t-1}$ computed from stage $t-1$, using the already received $\hat{\mathbf{z}}_1, \hat{\mathbf{z}}_2, ..., \hat{\mathbf{z}}_{t-1}$. Crucially, the encoder is equipped with a copy of the decoder, so having computed the same $\hat{\mathbf{x}}_{t-1}$, the encoder only encodes the information in $\mathbf{x}$ that is not present in $\hat{\mathbf{x}}_{t-1}$ (e.g., by encoding the *residual*, $\mathbf{x} - \hat{\mathbf{x}}_{t-1}$, in image compression). The resulting representation $\hat{\mathbf{z}}_t$ is sent to the decoder, which then uses $\hat{\mathbf{z}}_t$ to compute an improved tentative reconstruction $\hat{\mathbf{x}}_t$. This process continues, with $\hat{\mathbf{x}}_T$ declared the final data reconstruction $\hat{\mathbf{x}}$. Here, $f : \mathbf{x} \to \hat{\mathbf{z}}$ (similarly, g) is no longer

---

3. Unfortunately, this use of the term "encoder" for the function f of an autoencoder clashes with our definition of encoders $\mathbf{e}$ in Section 3. The "encoder" can also mean more abstractly the party initiating the data communication (and similarly, "decoder" can refer to the party receiving the data). The meaning is usually clear from the context.

implemented by a feedforward architecture, but rather a recurrent one, with $\hat{\mathbf{x}}_t$ being the recurrent state.

Such an approach embodies the idea of "analysis-by-synthesis", a classic model of perception and comprehension [95], and enables progressive compression whereby the data reconstruction $\hat{\mathbf{x}}_t$ improves as more information in $\hat{\mathbf{z}}_t$ is transmitted. Moreover, many video compression methods in Section 3.7 follow the same predictive coding paradigm, with $\mathbf{x} = [\mathbf{x}_1, ..., \mathbf{x}_T]$ being a sequence of video frames, and $\hat{\mathbf{z}}_t$ carrying the information in the reconstucted frame $\hat{\mathbf{x}}_t$.

We give a concrete example by Toderici et al. [96][93], who proposed some of the first recurrent neural architectures for progressive and variable-rate image compression. Here, the computation at each stage can be summarized as

$$\hat{\mathbf{z}}_t = [\![f_t(\mathbf{r}_{t-1})]\!], \mathbf{r}_t = \mathbf{x} - \hat{\mathbf{x}}_t, \hat{\mathbf{x}}_t = g_t(\hat{\mathbf{z}}_t) + \alpha \hat{\mathbf{x}}_{t-1};$$
$$\mathbf{r}_0 = \mathbf{x}, \hat{\mathbf{x}}_0 = \mathbf{0},$$

where $\mathbf{r}_t$, f_t, and g_t denote the residual vector, encoding transform, and decoding transform at time t, respectively, and $\alpha \in \{0, 1\}$ allows two different modes of operation. With $\alpha = 1$ ("additive reconstruction" mode), f_t and g_t can simply be a pair of CNNs (with a separate pair for each t), and are trained to additively correct the cumulative reconstruction at each stage. With $\alpha = 0$ ("one-shot reconstruction" mode), f_t and g_t are chosen to be stateful, and typically LSTM architectures, which are trained to directly predict the entire original image at each stage. Progressive and variable-rate image compression can then be achieved by controlling the number of steps T of the recursive computation.

3.3 Learned quantization and rate control

Neural networks have been used in image compression since before 1990 [3][5], but techniques were only recently developed to allow end-to-end training directly on a rate-distortion objective [96][92][14]. The main stumbling block has been the fact that the quantization operation and the discrete rate loss are not differentiable. As quantization maps (usually continuous) input to a discrete set, its derivative is zero almost everywhere and undefined at points of discontinuity. By the chain rule, the parameters of the encoder transform also receive zero gradient almost everywhere. Moreover, the rate loss, defined via the PMF $P(\hat{\mathbf{z}})$, also has no derivative w.r.t. the discrete representation $\hat{\mathbf{z}}$.

Below we survey the major approaches developed over the years for dealing with the non-differentiability problem, organized by how quantization is done. Since the issue of model training under quantization is intimately connected with minimizing or controlling the bit-rate (Eq. 25) of the encoder output $\hat{\mathbf{z}}$, we discuss both issues jointly. We note that although most of these techniques are developed for lossy compression, they are equally useful in lossless compression methods that make use of quantization [39], [40].

3.3.1 Binarization

Some of the earlier work quantized $\hat{\mathbf{z}}$ by element-wise binarization and used ad hoc approaches for rate estimation and control. Based on techniques for training binarized neural networks [97], Toderici et al. [96], [93] proposed stochastic binarization: each scalar element z of $\mathbf{z}$ is preprocessed to lie within $[-1, 1]$ (e.g., using point-wise $\tanh$ as the last layer

of f), and then stochastically rounded to -1 or 1 based on how close z is to either value:

$$[\![z]\!] := \mathrm{B}(z) = z + \epsilon, \quad \mathbb{P}(\epsilon) = \begin{cases} \frac{1+z}{2}, & \epsilon = 1 - z \\ \frac{1-z}{2}, & \epsilon = -1 - z \end{cases}$$

To backpropagate through stochasitic binarization, they used a Straight-through Estimator (STE) [98] and defined the gradient to be that of the identity function,

$$\frac{d}{dz} \mathrm{B}(z) := \frac{d}{dz} \mathbb{E}[\mathrm{B}(z)] = \frac{d}{dz} z = 1.$$

Toderici et al. [96], [93] trained the neural network model (f, g) to only minimize the distortion loss, relying on constraints on the dimension of the binary $\hat{\mathbf{z}}$ to implicitly control the rate. After training, a separate autoregressive entropy model (similar to a PixelRNN) is learned on the empirical distribution of $\hat{\mathbf{z}}$ to further reduce the bit-rate [93].

Li et al. [99] deterministically binarized $\mathbf{z}$ to $\{0, 1\}$ and used STE for backpropagation, optimizing a surrogate rate-distortion objective. For rate control, they introduced a learned masking mechanism to the encoder network to encourage sparsity in $\hat{\mathbf{z}}$, and optimized a surrogate rate loss defined in terms of the soft count of non-zeroed-out elements of $\hat{\mathbf{z}}$. After training, they fit a separate PixelCNN-style entropy model to further reduce rate, similar to [93].

3.3.2 Soft-to-Hard Vector Quantization

Agustsson et al. [100] proposed to use vector quantization with learned codebook values and introduced associated techniques for differentiable quantization and rate control. They considered the typical (hard) quantization operation in VQ (Sec. 3.1.2), mapping $\mathbf{z}$ to its closest codebook vector,

$$[\![\mathbf{z}]\!] := \mathrm{VQ}(\mathbf{z}, \mathcal{C}) = \mathbf{c}_j, \quad \text{with } j = \arg\min_i \|\mathbf{z} - \mathbf{c}_i\|,$$

where $\mathcal{C} = \{\mathbf{c}_i | i = 1, 2, .., M\}$ is a finite set of codebook vectors in $\mathbb{R}^N$ learned alongside the model. Agustsson et al. [100] proposed to approximate hard quantization by a differentiable *soft* quantization, via a linear combination of the codebook vectors weighted by how close they are to $\mathbf{z}$:

$$\mathrm{VQ}(\mathbf{z}, \mathcal{C}) \approx \mathrm{SoftQ}(\mathbf{z}, \mathcal{C}) := \sum_i \phi_i \mathbf{c}_i.$$

Here $\phi \in \Delta^{N-1}$ is a probability vector computed as the softmax of weighted distances, $\phi = \phi(\mathbf{z}, \mathcal{C}) := \mathrm{softmax}(-\sigma[\|\mathbf{z} - \mathbf{c}_1\|^2, ..., \|\mathbf{z} - \mathbf{c}_M\|^2])$, with $\sigma > 0$ a hyperparameter. In practice, due to the prohibitive computation cost of VQ, the proposed method is only applied independently to small blocks of $\mathbf{z}$. By annealing $\sigma \to \infty$ throughout training, soft quantization gradually approaches hard quantization, and a proper annealing schedule is needed to ensure effective training. For rate control, Agustsson et al. [100] essentially built an entropy model based on the empirical distribution of soft assignment probabilities.

Mentzer et al. [101] simplified the above technique by performing only scalar quantization and dispensing with the annealing procedure. They fixed σ at a constant (usually 1), and applied STE to differentiate through (hard) quantization using the gradient of soft quantization,

$$\frac{\partial}{\partial z} \mathrm{VQ}(z, \mathcal{C}) := \frac{\partial}{\partial z} \mathrm{SoftQ}(z, \mathcal{C}).$$

Mentzer et al. [101] furthermore trained a PixelCNN-style autoregressive entropy model end-to-end. To soften the non-differentiable discrete rate loss, they used the learned masking technique of Li et al. [99], but formed the surrogate rate loss based on the code length of non-zeroed-out elements of $\hat{\mathbf{z}}$ under the concurrently trained autogressive entropy model, instead of naive counts as used by Li et al. [99].

3.3.3 Uniform Quantization (UQ)

Popularized by Ballé and Theis et al. [92], [14], uniform quantization rounds each element of $\mathbf{z}$ to the closest integer,

$$[\![\mathbf{z}]\!] := \lfloor\mathbf{z}\rceil.$$

This can be viewed as a scalar version of the VQ approach, but with a fixed quantization grid equal to the set of integers. The assumption of a uniform quantization grid with width 1 can generally be justified by using a sufficiently flexible pair of transforms (f, g), which can warp the quantization grid in arbitrary ways if needed [92][17]. Compared to VQ, uniform quantization is cheap to compute. Moreover, by embedding the integer-valued discrete representation $\hat{\mathbf{z}}$ in $\mathbb{R}^N$, an entropy model can be conveniently specified in terms of a continuous density model, allowing for simpler differentiable rate surrogates than in approaches based on categorically distributed entropy models (e.g., [100][99], [101]). Such an entropy model P is defined by an underlying density p, exactly as in a discretized density model (Eq. 7),

$$P(\hat{\mathbf{z}}) := \int_{\hat{\mathbf{z}}+[-0.5,0.5)^N} p(\mathbf{v})d\mathbf{v}, \quad \forall\hat{\mathbf{z}} \in \mathbb{Z}^N. \quad (27)$$

We defer details on the choice of p to Section 3.3.4, and now discuss a few representative neural compression approaches based on this form of entropy model and integer-valued $\hat{\mathbf{z}}$. In the rest of this sub-section, $\mathbf{u} \sim \mathcal{U}\left([-0.5, 0.5)^N\right)$ is a r.v. with the uniform density $\mathcal{U}$ on the hypercube $[-0.5, 0.5)^N$.

UQ + STE. Theis et al. [14] proposed to train with uniform quantization and approximately differentiate through it by STE, using the identity gradient on the backward pass. For rate control, they optimized the same rate upper bound as on the LHS of Eq. 8, replacing the code length $-\log_2 P(\hat{\mathbf{z}})$ by the differentiable upper bound $\mathbb{E}_{\mathbf{u}}[-\log_2 p(\hat{\mathbf{z}} + \mathbf{u})]$.

Additive Uniform Noise. Ballé et al. [92] replace rounding with additive uniform noise for model training, i.e.,

$$\lfloor\mathbf{z}\rceil \approx \mathbf{z} + \mathbf{u}, \ \mathbf{u} \sim \mathcal{U}\left([-0.5, 0.5)^N\right).$$

Naively, one might simply substitute the above into the Lagrangian Eq. 26 and hope to obtain a reasonable training objective. However, the resulting code length, $-\log_2 P(f(\mathbf{x}) + \mathbf{u})$, does not yet make sense, as our entropy model P has only been defined over integers. It turns out the form of P (Eq. 27) offers a convenient solution: we can simply extend P from $\mathbb{Z}^N$ to all of $\mathbb{R}^N$, by convolving the underlying density p with the uniform noise $\mathbf{u}$, i.e.,

$$\tilde{p} := p * \mathcal{U}\left([-0.5, 0.5)^N\right). \quad (28)$$

It's easy to see that $\tilde{p}$ agrees with P on all integer points, and serves as a smoothed relaxation of P which defines a surrogate gradient with respect to its input. Replacing P

by $\tilde{p}$ in Eq. 26, and taking expectation with respect to the uniform noise $\mathbf{u}$, we obtain the surrogate training objective,

$$\mathbb{E}_{\mathbf{x}\sim p_{data},\mathbf{u}}[-\log_2 \tilde{p}(f(\mathbf{x}) + \mathbf{u}) + \lambda\rho(\mathbf{x}, g(f(\mathbf{x}) + \mathbf{u}))], \quad (29)$$

which is now differentiable with respect to all components of the model, and can be simply estimated by sampling. Although motivated as an approximation to the rate-distortion cost under uniform quantization (Eq. 26), Eq. 29 can be shown [17][102] to exactly equal the rate-distortion cost of compression with dithered quantization (i.e., quantization with a random offset, $[\![\mathbf{z}]\!] := \lfloor\mathbf{z} - \mathbf{u}\rceil + \mathbf{u}$); see Section 3.4.

It is instructive to consider the density model p as approximating the distribution of the *continuous* representation $\mathbf{z} = f(\mathbf{x})$ as induced by $\mathbf{x} \sim p_{data}$ and the analysis transform f. Indeed, suppose $\mathbf{z}$ is distributed according to p, then the distribution of $\hat{\mathbf{z}} = \lfloor\mathbf{z}\rceil$ is exactly captured by the entropy model P defined by Eq. 27. Moreover, if we define the "noisy quantization" by the random variable $\tilde{\mathbf{z}} := \mathbf{z} + \mathbf{u}$, then its induced density (given $\mathbf{z} \sim p$) is precisely $\tilde{p}$ from Eq. 28. It turns out under this perspective, the surrogate Lagrangian based on additive noise (Eq. 29) bears a close relation to the NELBO objective of a particular type of VAE, where $\tilde{\mathbf{z}}$ is the latent variable. Consider, for simplicity, that ρ is the squared difference, $\rho(\mathbf{x}_1, \mathbf{x}_2) = \|\mathbf{x}_1 - \mathbf{x}_2\|^2$. Then Eq. 29 can be shown [92], [14] to be equal to an NELBO,

$$\mathbb{E}_{\mathbf{x}\sim p_{data}} \mathbb{E}_{q(\tilde{\mathbf{z}}|\mathbf{x})}[-\log_2 \tilde{p}(\tilde{\mathbf{z}})+\log_2 q(\tilde{\mathbf{z}}|\mathbf{x})-\log_2 p(\mathbf{x}|\tilde{\mathbf{z}})]+\text{const},$$

where $\tilde{p}(\tilde{\mathbf{z}})$ plays the role of a prior, $q(\tilde{\mathbf{z}}|\mathbf{x})$ is a fully factorized uniform posterior density centered at $\mathbf{z} = f(\mathbf{x})$, and $p(\mathbf{x}|\tilde{\mathbf{z}})$ is a Gaussian likelihood model with mean equal to the reconstruction $\hat{\mathbf{x}} = g(\tilde{\mathbf{z}})$, and diagonal covariance controlled by λ. With this choice of distributions, sampling from the uniform posterior q via the reparameterization trick is precisely equivalent to adding uniform noise to the encoding; the prior term of the NELBO then equals the expected rate loss in Eq. 29, the posterior entropy term is constant (in fact, 0), and the log-likelihood term equals a squared distortion loss.

Discrete Latents and Stochastic Gumbel Annealing. There is an alternative perspective on neural lossy compression that also connects optimizing an expected rate-distortion loss to training a probabilistic autoencoder with *discrete* latent variables [103], [16]. Under this perspective, given data sample $\mathbf{x}$, we use a stochastic encoder to compute a distribution over the discrete encoding, denoted by $q(\hat{\mathbf{z}}|\mathbf{x})$. We then randomly sample a $\hat{\mathbf{z}}$ value from this distribution and transmit it losslessly to the receiver. The expected rate-distortion cost of this compression procedure is then

$$\mathbb{E}_{\mathbf{x}\sim p_{data}} \mathbb{E}_{\hat{\mathbf{z}}\sim q(\hat{\mathbf{z}}|\mathbf{x})}[-\log_2 P(\hat{\mathbf{z}}) + \lambda\rho(\mathbf{x}, g(\hat{\mathbf{z}}))]. \quad (30)$$

As before, we can interpret the distortion term to correspond to a suitably chosen negative log-likelihood, i.e., $\lambda\rho(\mathbf{x}, g(\hat{\mathbf{z}})) = -\log_2 p(\mathbf{x}|\hat{\mathbf{z}}) + \text{const}$. Then the above loss function has the form the NELBO of a VAE, but without the usual posterior entropy term; and unlike the VAE obtained from additive uniform noise (see previous paragraph), the latent variable $\hat{\mathbf{z}}$ here is discrete. As pointed out by Habibian et al. [103], this loss is in fact an upper bound on the usual NELBO: for each $\mathbf{x}$, the expected rate, a cross-entropy, $\mathbb{E}_{q(\hat{\mathbf{z}}|\mathbf{x})}[-\log_2 P(\hat{\mathbf{z}})]$, upper bounds the

usual $KL(q(\hat{\mathbf{z}}|\mathbf{x})\|P(\hat{\mathbf{z}}))$, with the gap equal to the entropy $\mathbb{H}[q(\hat{\mathbf{z}}|\mathbf{x})]$. The upper bound becomes tight for an optimal encoder, which deterministically places all the mass of $q(\hat{\mathbf{z}}|\mathbf{x})$ on the $\hat{\mathbf{z}}$ value that minimizes Eq. 30 for each $\mathbf{x}$. Note that generally, the divergence $KL(q(\hat{\mathbf{z}}|\mathbf{x})\|P(\hat{\mathbf{z}}))$ is only an ideal rate that is achieved asymptotically by a likelihood encoder (see Section 3.4.2).

Based on this perspective, Yang et al. [16] considered a variational distribution $q(\hat{\mathbf{z}}|\mathbf{x})$ parameterized by a continuous vector $\boldsymbol{\mu} \in \mathbb{R}^N$ (optionally predicted by the inference network), such that the distribution is concentrated on a small number of integer vectors near $\boldsymbol{\mu}$. The probability for each integer configuration of $q(\hat{\mathbf{z}}|\mathbf{x})$ depends inversely on its distance to $\boldsymbol{\mu}$, similarly to the softmax formulation of Agustsson et al. [100]; a similar temperature hyperparameter is annealed throughout optimization to make q become increasingly deterministic, such that sampling from q mimics hard rounding. To optimize w.r.t. the parameter $\boldsymbol{\mu}$, the Gumbel-softmax trick [104], [105] is used to differentiate through samples of q. The discrete entropy model P is replaced by its continuous extension $\tilde{p}$ (Eq. 28) for gradient-based optimization, as in the uniform noise approach. The resulting method, Stochastic Gumbel Annealing (SGA), is applied to improve the compression performance of pre-trained models at test time [16].

Tsubota et al. [106] further applied a version of SGA for end-to-end training, using STE instead of the Gumbel-softmax trick to differentiate through sampling $\hat{\mathbf{z}} \sim q$ (which we refer to as SGA+STE), and obtained improved R-D performance compared to the UQ+STE approach.

Comparisons. Empirical results [107], [20], [108] suggest that it is beneficial to train with different approximations for optimizing the distortion v.s. the rate terms of the R-D loss (Eq. 26). A recent empirical comparison of combinations of various approaches [106] confirms this, showing that it is best to combine a rounding-based approximation (SGA+STE, UQ+STE) for the distortion term, and a uniform-noise-based approximation (additive uniform noise, dithered quantization [109]) for the rate term.

3.3.4 Entropy models

Various entropy models have been proposed to reduce the bit-rate and improve the rate-distortion performance of neural lossy compression, using largely the same modeling ideas as for lossless compression.

In most approaches before uniform quantization, such as binarization or VQ with learned codebooks, an autoregressive entropy model (a.k.a., "context model") is most often used, either with a PixelCNN-like neural model [99], [93], [101], or an off-the-shelf adaptive entropy coder [100].

More possibilities have been explored in approaches based on uniform quantization, where the entropy model can be conveniently parameterized in terms of a density model p ("prior density") as in Eq. 27. Perhaps the simplest choice is a fully-factorized p, resulting in a factorized entropy model. Each marginal of p is typically parameterized as a mixture distribution [14], or indirectly as the derivative of a deep CDF model [41] (exploiting the relation in Eq. 9).

Going beyond factorized entropy models, recent research has explored latent-variable modeling, autoregressive modeling, and their combination, to increase the flex-

ibility of the prior density p and improve the compression rate [41], [42], [20]. The basic latent variable model approach, commonly referred to as the *hyperprior* approach [41], expresses the entropy model's underlying density through an additional hierarchy of latent variables $\mathbf{h}$ ("hyper-latents"),

$$\mathbf{h} \sim p(\mathbf{h}), \hat{\mathbf{h}} = \lfloor \mathbf{h} \rceil;$$
$$\mathbf{z}|\hat{\mathbf{h}} \sim p(\mathbf{z}|\hat{\mathbf{h}}), \hat{\mathbf{z}} = \lfloor \mathbf{z} \rceil.$$

The hyperprior density, $p(\mathbf{h})$, is typically parameterized as in a factorized entropy model, while $p(\mathbf{z}|\hat{\mathbf{h}})$ is a density (e.g., factorized Gaussian) whose parameters are predicted from $\hat{\mathbf{h}}$ by a neural network ("hyper-decoder"). Crucially, note that the prior density of $\mathbf{z}$ is conditioned on the discrete $\hat{\mathbf{h}}$, as the hyper-latents must be discretized and entropy-coded first at compression time. The information transmitted in the hyper-latents is known as *side information* in traditional data compression, and lets the sender and receiver dynamically select an entropy model based on the content of the input data. To train such an entropy model, the rate loss (Eq. 25) is modified to account for the side-information, replacing $-\log_2 P(\hat{\mathbf{z}})$ by the joint information content $-\log_2 P(\hat{\mathbf{z}}, \hat{\mathbf{h}}) = -\log_2 P(\hat{\mathbf{h}}) - \log_2 P(\hat{\mathbf{z}}|\hat{\mathbf{h}})$; the same techniques from Section 3.3.3 can then be used to differentiate through quantization and rate loss. Empirically, the hyperprior considerably reduces the overall bit-rate of a factorized entropy model, with the side-information comprising a small percentage of the overall rate [41].

The bit-rate can be further improved by additionally modeling $\hat{\mathbf{z}}$ autoregressively similarly to a PixelCNN [42], but results in serial and hence slower decoding. To address this, Minnen et al. [20] proposed to instead use channel-wise (instead of spatial) autoregressive conditioning, significantly speeding up (de)compression without harming the rate-distortion performance. Compared to an autoregressive model, a latent-variable entropy model has the advantage of parallel encoding/decoding via (conditionally) factorized distributions, but entails transmitting side-information, similar to the two-part code in lossless compression (Section 2.3.1). Yang et al. [16] applied bits-back coding to reduce the transmission of side-information in a hyperprior model.

Regardless of the choice of an entropy model, the sender and receiver must agree on the exact same probabilities for entropy coding (such as AC) to operate correctly. This can be a stringent requirement when the entropy models (e.g., the conditional model $P(\hat{\mathbf{z}}|\hat{\mathbf{h}})$) are computed dynamically, especially in the face of round-off errors from floating point arithmetics, and/or non-deterministic GPU operations. We refer readers to Ballé et al. [110] for more details on this issue, and a potential solution based on integer arithmetics.

3.4 Compression without quantization

The non-differentiability of quantization has hindered end-to-end training of lossy compression models, and the various methods in Section 3.3 replace quantization by a differentiable surrogate at training time. The mismatch between "soft" quantization during training and "hard" quantization at test time generally results in sub-optimal performance [16]. Annealing can alleviate the problem [100][16][102], but may suffer high-variance gradients as the approximation

approaches quantization, or require tuning. Researchers have therefore explored alternative compression approaches that do not entail quantization during training.

Yang et al. [111] considered quantizing the mode of the variational posterior $q(\mathbf{z}|\mathbf{x})$ in a Bayesian statistical model, in both data and model compression settings. Their method exploits posterior variance to reduce the bit-rate cost for more "uncertain" latent dimensions (a feature shared with bits-back coding). By decoupling model training and quantization, the method also naturally lends to variable-rate compression, but is generally out-performed by end-to-end trained image compression methods at lower bit-rates.

Quantization can, in fact, be avoided entirely, if we do not insist on transmitting a fixed value of continuous representation $\mathbf{z}$. Instead, we may transmit a random sample of $\mathbf{z}$ that is nonetheless informative about the data $\mathbf{x}$. Recent research has investigated efficient communication of a continuous but stochastic representation $\mathbf{z} \sim q(\mathbf{z} \mid \mathbf{x})$ directly over a digital channel [112], a problem more generally recognized as *channel simulation* [113][114], *reverse channel coding* [112][102], or *relative entropy coding* [115].

Bits-back coding (Section 2.3.2) seems like a natural candidate for this problem as it also uses a stochastic encoder. Unfortunately, it requires the exact data $\mathbf{x}$ to be eventually available to the decoder to achieve full "bits-back" efficiency, and therefore is only directly applicable to lossless compression, and not a general solution to reverse channel coding.

Li & El Gamal [114] showed that is is possible to communicate $\mathbf{z}$ at an average coding cost of at most

$$I[\mathbf{x},\mathbf{z}] + \log_2(I[\mathbf{x},\mathbf{z}] + 1) + 5$$

bits. That is, the coding cost is close to the information contained in $\mathbf{z}$. However, they also showed that in general it is not possible to significantly reduce the coding cost. Even for optimal encoders and decoders we may therefore have to pay an overhead which is logarithmic in the mutual information. However, this overhead is relatively small if the mutual information is large.

One way to increase the mutual information (and thus reduce the relative overhead) is to communicate more information at once (for example, by bundling multiple frames of a video). Unfortunately, it can be computationally very expensive to do so. Agustsson & Theis [102] showed that there is no general reverse channel coding algorithm whose computational cost is polynomial in the information content. If we want to transmit large amounts of information at once using as few bits as possible, then this may only be possible by spending a lot of computation. Nevertheless, some distributions can be communicated efficiently, both computationally and with low overhead.

In the following, we will review two strategies for communicating stochastic information. One is a simple and efficient approach for simulating channels with additive uniform noise, and one is a general approach for communicating samples of arbitrary distributions. For a more thorough introduction to reverse channel coding, see Theis & Yosri [116].

3.4.1 Dithered quantization

Consider a latent representation $\mathbf{z}$ which is the output of a neural network followed by additive uniform noise, i.e.,

$$\mathbf{y} := f(\mathbf{x}), \qquad \mathbf{z} := \mathbf{y} + \mathbf{u}, \qquad (31)$$

where $\mathbf{u}$ is a vector of uniform noise with values between -0.5 and 0.5. It turns out that we can efficiently communicate an instance of $\mathbf{z}$ using an old technique called *dithered* or *universal quantization* [117][85]. The key insight is that

$$\mathbf{k} := \lfloor \mathbf{y} - \mathbf{u}' \rceil \quad \implies \quad \mathbf{k} + \mathbf{u}' \overset{d}{=} \mathbf{y} + \mathbf{u}, \qquad (32)$$

where $\mathbf{u}'$ is another vector of independent uniform noise. That is, subtracting uniform noise, rounding, and then adding uniform noise back is distributionally equivalent to adding noise directly. We can exploit this for the communication of a sample of $\mathbf{z}$ as follows. The encoder computes $\mathbf{k}$ and entropy encodes it. The decoder receives $\mathbf{k}$ and simply adds $\mathbf{u}'$. This assumes that both the encoder and decoder have access to the same $\mathbf{u}'$, e.g., by sharing a random seed.

The entropy of $\mathbf{k}$ turns out to be exactly $I[\mathbf{y},\mathbf{z}]$ [118]. The coding cost thus has two very useful properties. First, it is equal to the amount of information transmitted. That is, entropy coding $\mathbf{k}$ is a statistically efficient strategy for communicating an instance of $\mathbf{z}$. Second, the mutual information is the expectation of a differentiable function in $\mathbf{y}$ so that we can easily optimize encoders using backpropagation [102].

3.4.2 Minimal random coding

While dithered quantization can be computationally and statistically efficient, it is only able to communicate certain simple distributions. Several general algorithms have been developed to communicate a sample from arbitrary distributions [119][120][121][114][122][116]. Here we are describing one algorithm based on importance sampling. In information theory, it is known as the *likelihood encoder* [121][123]. In machine learning, it has recently been introduced as *minimal random coding* [122][115].

Assume both the encoder and decoder have access to $p(\mathbf{z})$. The encoder generates N examples $\mathbf{z}_n \sim p(\mathbf{z})$ and forms importance weights $w_n = q(\mathbf{z}_n \mid \mathbf{x})/p(\mathbf{z}_n)$ for a target distribution $q(\mathbf{z} \mid \mathbf{x})$. It then randomly samples an index k using the normalized importance weights,

$$P(n) = \frac{w_n}{\sum_m w_m}, \quad k \sim P. \qquad (33)$$

The index is uniformly distributed and encoded using $\log_2 N$ bits. The decoder receives k and reconstructs $\mathbf{z}_k$. It can do this if the encoder used a pseudorandom number generator to generate the candidates, and the seed is known to the decoder. Havasi et al. [122] showed that if the number of samples is

$$N = 2^{D_{\mathrm{KL}}[q(\mathbf{z}|\mathbf{x}) \,\|\, p(\mathbf{z})]+t}, \qquad (34)$$

then under reasonable assumptions, estimates based on $\mathbf{z}_k$ will be similar to estimates based on $\mathbf{z}$ for $t > 0$. Havasi et al. [122] applied minimal random coding to model compression, while Flamich et al. [115] used it for image compression. Theis & Yosri [116] showed that the coding cost of minimal random coding can be further reduced without any loss in quality.

3.4.3 Stochastic versus deterministic coding

Communication of information without any quantization requires a certain level of noise to be present. Without noise or quantization, there would be no limit to the amount of information we could send through the bottleneck of an autoencoder. This raises the question of whether a deterministic encoder with quantization or a stochastic encoder is better. Ballé et al. [17] argue that we can always improve on dithered quantization with a deterministic encoder when performance is measured by a rate-distortion trade-off. Theis & Agustsson [124] extended this argument to arbitrary stochastic encoders. That is, when we care about a rate-distortion trade-off, the best stochastic encoder is likely to perform worse than the best deterministic encoder. However, Theis & Agustsson [124] also showed by example that when we additionally care about the realism of reconstructions (discussed in Section 3.5), stochastic encoders can perform significantly better than deterministic ones. Which one is better therefore depends on the setting of interest.

3.5 Perceptual losses

Neural networks are only as good as the losses they are trained for. While in lossless compression the objective is clear – namely to minimize the required number of bits to represent the data – the story is a lot more complicated when we turn to lossy compression. Here we need to make decisions about which information to sacrifice in order to save additional bits. In typical forms of media compression, however, the goal is to make any reconstruction errors as imperceptible as possible. This raises complicated questions about how our brains perceive differences between signals.

3.5.1 Background

We can distinguish between two types of distortions, namely *full-reference metrics* and *no-reference metrics*. The former is a function which takes an image and its reconstruction as input while the latter only looks at the reconstruction to make a judgement about its quality. These can be motivated by two corresponding types of quality measures involving humans. *Mean-opinion scores* (MOS) [125] are measured by having raters judge reconstructions on a scale from 1 (bad) to 5 (excellent). Since raters are only provided with the reconstructions, their judgments can be viewed as the output of a no-reference metric. Many other *image quality assessments* (IQAs) evaluate perceptual quality without reference to the original data [126], but MOS is the most widely used measure due to its simplicity. In contrast, *degradation MOS* (DMOS) asks raters for a judgment based on both the unprocessed and the reconstructed data [125], and thus is more akin to a full-reference metric.

In addition to distortions, we may consider *divergences* which depend on the probability distribution of the data and the marginal distribution of reconstructions. Driven by the success of *generative adversarial networks* (GANs) [6] in producing realistic looking images, divergence optimization has become an important topic in neural compression.

3.5.2 Perceptual distortions

In this section we explore some of the metrics that are most likely to be encountered in the current literature on neural compression. However, there is a much larger body of potentially relevant work on IQAs and more broadly on perception that we will have to ignore here. For example, *VMAF* [127][128] is a full-reference metric which is frequently used to evaluate the quality of video in industry but it has not yet found widespread use in the neural compression community.

Mean-squared error (MSE) and peak signal-to-noise ratio (PSNR) are frequently used in neural compression but do not predict perceived quality well [129]. Another criterion widely used in machine learning and beyond is the structural similarity index (SSIM) [130]. SSIM has been shown to correlate better with human perception and has been extensively studied and extended. The extension most commonly found in neural compression papers is the multi-scale SSIM (MSSSIM) [131] which evaluates SSIM at multiple resolutions and combines them multiplicatively.

While MSE and PSNR are computed pixel-wise, SSIM is computed from small image patches. Let $\mathbf{x}$ and $\mathbf{y}$ be two aligned grayscale image patches extracted from an image and its reconstruction, respectively. Further, let $\mu_\mathbf{x}, \sigma_\mathbf{x}$, and $\sigma_\mathbf{xy}$ represent the average pixel value, the standard deviation and the covariance of pixel values as measured from these patches. Using these quantities, we define

$$l(\mathbf{x}, \mathbf{y}) = \frac{2\mu_\mathbf{x}\mu_\mathbf{y}}{\mu_\mathbf{x}^2 + \mu_\mathbf{y}^2}; \; c(\mathbf{x}, \mathbf{y}) = \frac{2\sigma_\mathbf{x}\sigma_\mathbf{y}}{\sigma_\mathbf{x}^2 + \sigma_\mathbf{y}^2}; \; s(\mathbf{x}, \mathbf{y}) = \frac{\sigma_\mathbf{xy}}{\sigma_\mathbf{x}\sigma_\mathbf{y}}.$$

(Small positive constants are added to the numerator and denominator of each expression for numerical stability.) The structural similarity function s measures correlation, while the luminance function l and contrast function c are chosen to respond to *relative* changes in luminance or contrast. These functions will not change much if, for example, both $\mu_\mathbf{x}$ and $\mu_\mathbf{y}$ are scaled by the same factor. This is consistent with Weber's law of how the human visual system perceives changes in these parameters [131]. SSIM is defined as

$$\text{SSIM}(\mathbf{x}, \mathbf{y}) = l(\mathbf{x}, \mathbf{y})^\alpha c(\mathbf{x}, \mathbf{y})^\beta s(\mathbf{x}, \mathbf{y})^\gamma,$$

where α, β, γ are additional parameters which control the relative importance of the factors (typically set to 1). Note that $\text{SSIM}(\mathbf{x}, \mathbf{x}) = 1$. To compute a single value for an entire image, one approach is to use a sliding window (e.g., 8×8 pixels) and then to average SSIM values. MS-SSIM instead uses a smooth windowing approach to compute local statistics in order to avoid blocking artifacts [131]. SSIM is defined for grayscale images. In the neural compression literature, SSIM is typically applied separately to RGB channels and the resulting values averaged to evaluate color images.

SSIM has been shown to perform significantly better at predicting human judgments than MSE on common distortions such as blurriness, noise or blocking artifacts [130]. However, its limitations are also well documented and it tends to fail for reconstructions produced by generative compression approaches [132][133].

"When a measure becomes a target, it ceases to be a good measure" [134]. In line with this adage, directly optimizing neural networks for MS-SSIM offers mixed results when compared to MSE in terms of perceptual quality [41]. Unlike many applications of IQA, a metric has to make meaningful predictions for all conceivable distortions to be useful as a target in neural compression and cannot have any blind

spots. Ding et al. [135] recently compared a large number of IQA methods and found that many were unsuitable for direct optimization.

A common approach to the design of more sophisticated distortions is to rely on deep neural networks which perform well in some other vision task. Typically, these distortions take the form

$$\rho_\Phi(\mathbf{x}, \mathbf{y}) = \rho(\Phi(\mathbf{x}), \Phi(\mathbf{y})), \tag{35}$$

where Φ is some representation derived from the hidden activations of a neural network and d is typically the MSE. Gatys et al. [136] compellingly demonstrated the ability of such metrics to capture semantic content at different levels of abstraction in their seminal paper on neural style transfer. Bruna et al. [137] used distortions derived from VGG [138] and scattering networks [139] and applied them to the task of super-resolution, which can be viewed as a simpler form of neural compression with a fixed encoder. They found that these distortions lead to sharper reconstructions than MSE but can also cause artifacts.

Zhang et al. [140] further investigated the efficacy of distortions based on VGG and found that they can significantly outperform SSIM on a range of artifacts including those generated by neural networks. They further proposed the *learned perceptual image patch similarity* (LPIPS). LPIPS uses pretrained classifiers such as AlexNet [141] or VGG [138] but its parameters are finetuned in a supervised manner to match human responses. As an alternative, Bardwaj et al. [142] recently showed that representations learned in a completely unsupervised manner can be as effective as LPIPS and proposed the *perceptual information metric* (PIM). Here, Φ was learned using a contrastive loss.

3.5.3 No-reference metrics

While no-reference metrics are rarely used as training targets in the current neural compression literature, they are sometimes used for evaluation [133]. The *natural image quality evaluator* (NIQE) [143], for example, extracts nonlinear features from image patches sampled from a test image. It then fits a Gaussian distribution to these features and compares it to a Gaussian distribution fitted to features extracted from natural images. Many extensions of NIQE have been proposed and used in the IQA literature [144].

Deep IQA [145] samples 32x32 image patches from a test image and uses a convolutional neural network to predict perceptual quality judgments. The predictions for different patches are averaged to yield a single score for an image. The parameters of the network were trained in a supervised manner on the LIVE dataset [146] which only contains 981 distorted versions of 29 reference images. To augment this dataset and to reduce overfitting, Kim et al. [147] pretrained a neural network to predict pixel-wise distortions before training on the LIVE dataset.

3.5.4 Divergences and adversarial networks

An image compressor which always outputs a fixed image of high perceptual quality would score high in terms of any no-reference metric and consume zero bits. However, for a useful compressor of natural images, we expect a *diverse* distribution of reconstructions. Such properties can be assessed with *divergences*, measuring the deviation between the data distribution and the distribution of reconstructions. Requirements on a divergence d are $d[p, q] \geq 0$ and $d[p, q] = 0 \iff p = q$ for all distributions p, q, and a divergence need not be symmetric. Examples include the Kullback-Leibler divergence (KLD), the Jensen-Shannon divergence (JSD), or the total variation distance (TVD).

Divergences are sometimes described as either *zero-avoiding* or *zero-forcing* [148]. Zero-avoiding divergences assign a high penalty to models which assign zero probability to events ($q(\mathbf{x}) = 0$) which have positive probability under the reference distribution ($p(\mathbf{x}) > 0$). They are also called *mode-covering* divergences since they encourage models to assign probability mass to all modes of a distribution. Examples include the KLD or the χ^2-divergence. On the other hand, zero-forcing divergences assign a high penalty to model distributions which assign positive probability ($q(\mathbf{x}) > 0$) to events which have zero probability ($p(\mathbf{x}) = 0$). These are also called *mode-seeking* divergences since the resulting models tend to ignore some of the modes of distributions with multiple peaks. An examples is the reverse KLD (Eq. 6 with P and Q switched). Zero-forcing divergences are especially useful for capturing realism since they discourage models from generating implausible reconstructions.

Optimizing divergences of high dimensional distributions is challenging. Nevertheless, approximations optimized by generative adversarial networks (GANs) have proven useful in practice [6][149]. Weighted combinations of distortions and adversarial losses have produced very promising results in neural compression and related image reconstruction tasks [132][150][151][152][133]. For example, Agustsson et al. [152] were able to train autoencoders achieving much more detailed reconstructions at extremely low bit-rates than advanced classical codecs by targeting a perceptual distortion loss $\mathcal{L}_\rho$ and a least-squares adversarial loss (LSGAN) [153] $\mathcal{L}_D$, using the combined loss function

$$\sup_{D \in \mathcal{D}} \mathcal{L}_D(f, g) + \beta \mathcal{L}_\rho(f, g), \tag{36}$$

where D is a discriminator (adversary) network, and

$$\mathcal{L}_D(f, g) := \mathbb{E}[(D(X) - 1)^2 + D(g([\![f(X)]\!], Z))^2], \tag{37}$$
$$\mathcal{L}_\rho(f, g) := \mathbb{E}[\|\Phi(X) - \Phi(g([\![f(X)]\!], Z))\|^2]. \tag{38}$$

Here, $[\![\cdot]\!]$ is a quantizer mapping the output of the encoder to a finite number of values. Instead of explicitly optimizing a bit-rate, the bit-rate was controlled by limiting the number of values of the quantizer. In addition to the encoder's outputs, the decoder receives independent noise Z as input. The feature representation Φ is a combination of pixels and VGG feature activations. Interestingly, the χ^2-divergence approximated by the LSGAN loss exhibits even stronger mode-covering behavior than the KLD. This does not seem to prevent LSGAN from being able to produce sharp images, which may be further evidence that adversarial losses do not always behave like the divergences they target [154].

Divergences are not just used for training but also for evaluating neural compression results. In particular, the Frechet inception distance (FID) [155] measures the squared Wasserstein-2 distance between the data and reconstructions in the feature space of the *inception-v3* network [156], approximating both distributions as multivariate Gaussian.

Both FID and NIQE (Section 3.5.3) measure the distance between two Gaussian distributions. However, while NIQE estimates the distribution of features *within* a single image, FID measures the distribution of features *across* many different images.

3.5.5 Perception-distortion trade-off

An important question for neural compression is whether divergences are needed at all. Could we achieve the same results with just a distortion? Optimizing MSE, SSIM and even neural-network-based losses tend to produce artefacts but perhaps these will disappear as perceptual distortions improve. A strong counterargument to this hope was given by Blau & Michaeli [157]. They showed that *any* distortion is going to produce artefacts for some data unless the compressed representation allows us to reproduce the inputs perfectly. That is, for any lossy codec, the optimal reconstruction $\hat{x}$ of x optimized for the expectation of a given distortion will not preserve the data distribution [157, Theorem 1]. Note that this limitation does not apply if we are allowed to optimize divergences since then we can achieve perfect realism by requiring that all admissible decoders produce reconstructions such that $d[p_{\hat{x}}, p_x] = 0$ for some divergence d, at least in theory. Blau & Michaeli [157] also showed that the achievable divergence can only increase when we demand lower levels of distortion. This makes sense, as the set of available decoders shrinks as we impose stronger constraints on them. Counterintuitively, however, this means that minimizing distortion can have the effect of reducing the realism of reconstructions. Blau & Michaeli [157] called this the *perception-distortion trade-off*, that is, a small distortion limits the achievable realism and a low divergence (high realism) limits the achievable distortion. However, different choices of distortions can affect the distortion-realism differently [158] [132] [157].

3.6 Feature compression

As more data is communicated and processed by machines, a natural question arises whether we can optimize compression toward a supervised goal, such as classification (rather than optimizing for perceptual quality). For example, Yang et al. [159] studied the effect of JPEG artefacts on classification accuracy, while Singh et al. [160] studied the trade-off between low bit-rates and classification accuracy using similar models as in learned image compression. Matsubara et al. [161] demonstrated the benefits of knowledge distillation in this context. Dubois et al. [162] introduced a supervised compression framework suitable to a multitude of tasks invariant under a set of transformations. In addition to accuracy, computational decoding efficiency is a big concern when developing codecs for ML models. Training modern classifiers requires the decoding of millions of images or video frames. For example, instead of decoding JPEG images to pixels, Bulla et al. [163] only decoded the DCT coefficients and fed them directly to a classifier.

3.7 Video compression

While deep generative modeling has impacted image compression early on [11], its application to *video* compression began more recently (circa 2018), likely due to the additional complexity in modeling and computing with videos.

A typical video codec consists of two steps: motion compensation and residual compression. The idea behind motion compensation is to predict the next frame in a video based on previous frames. Traditionally, motion compensation relied on block motion estimation (i.e., matching entire patches in videos and memorizing compressed displacement vectors). By contrast, neural approaches typically directly predict the displacement fields of pixels between adjacent frames. If the predicted displacement field is 'simple', e.g., sparse, it can be efficiently compressed. Since certain aspects in a video can not easily be predicted, the (typically sparse) residual is separately compressed using image compression models (classical or neural).

Recently proposed neural video codecs differ in design choices of the predictive model (e.g., stochastic vs deterministic) and the residual compression scheme (e.g., compression in latent space vs. pixel space). Another fundamental design choice is to either consider the low-latency setup in which a video has to be encoded and decoded on a frame-by-frame level, or the offline setup, in which case the video is encoded as a whole (using knowledge of future frames). For example, the offline setup may be adequate for video streaming services, while the online setup may be more suitable for video conferencing. Another line of research investigates hybridizing classical and neural codecs [18].

One of the earliest approaches to joint prediction and residual compression based on convolutional architectures was [164], which still used a traditional block-based motion estimation approach. For offline compression, [165][166] formulated the video compression problem as a frame interpolation problem. Here, a subset of "key frames" are compressed as images, and the intermediate frames reconstructed based on video interpolation techniques.

Most neural compression approaches currently focus on the low-latency (online) setup [167][168][108][169][170][171]. These approaches can be interpreted as generative models for frame sequences. Han et al. [167] and Habibian et al. [103] first adapted the neural image compression framework of Ballé et al. [13] to video data, framing it in a variational inference context. While Han et al. [167] proposed to encode the frame sequence using the predictive next-frame distribution of a stochastic recurrent neural network (eliminating the need to separately compress residuals) and adding a global latent variable that played a similar role as a key frame in traditional compression, Haibibian et al. [103] used 3D convolutions and explored structured priors such as PixelCNNs [52] for lower bit-rates at the expense of increased runtime.

In subsequent work, the separation of motion estimation and residual compression dominated and led to improvements over classical video codecs such as HEVC. Lu et al. [168] adopted a hybrid architecture that combined a pretrained Flownet [172] and residual compression. Rippel et al. [173] proposed a motion estimation approach with long-term memory and adaptive rate control.

Another noteworthy innovation are scale-space flows. Agustsson et al. [108] used learned optical flows and warping to predict the next frame in sequence, however, it does so by adding a "scale" dimension to the optical flow field. This

dimension allows the model to adaptively blur the source based on how well the next frame is predicted. A general framework for low-latency video compression was recently introduced by Yang et al. [174]. The paper also showed that the frame reconstruction for models such as [108] could be improved by introducing a scale parameter that mediates between the autoregressive prediction and the compressed residual (in a similar way as how RealNVP improves over NICE [175], [176]), as well as by using non-factorized priors.

4 DISCUSSION AND OPEN PROBLEMS

Neural compression is a rapidly growing field making significant strides in both lossless and lossy compression. While neural approaches to image compression barely beat JPEG 2000 in 2016 [14] [13], they already outperformed the best known handcrafted codecs in 2018 [177]. And in the *Challenge on Learned Image Compression* of 2021, classical codecs did not even make it into the top 10. Similarly, the leading codec in the *Large Text Compression Benchmark* relied solely on neural networks to predict text [47].

Nevertheless, many practical and theoretical challenges remain. Chief among them is the issue of computational complexity. While neural networks offer remarkable compression performance, they demand significantly higher computation than traditional codecs. Research into more efficient neural architecture and coding schemes will be crucial for the wider deployment of neural compression.

Many open questions also remain in the design of loss functions in lossy compression. For example, it is poorly understood to which extent divergences and adversarial approaches are needed for realism, or whether realism could also be achieved through well crafted distortions and no-reference metrics. Adversarial losses also continue to pose challenges for tuning and optimization and no loss has yet emerged which can be trusted to reliably judge the perceptual quality of reconstructions in training and evaluation.

The use of quantization continues to cause a mismatch between training and test time performance, and how much this affects compression performance is still not clearly understood. Reverse channel coding is a promising alternative which eliminates the need for quantization, but has only recently been considered in neural compression [116]. Open questions include the design of efficient coding schemes and the impact these schemes have on performance when compared to approaches based on quantization.

Finally, all the above issues come to the fore when we apply neural compression to more complex data such as video, VR content, or even non-Euclidean data. Besides making it computationally feasible, effectively compressing such data likely also requires advances in generative modeling, as well as in the design of new distortion or other loss functions.

REFERENCES

[1] C. Dong, C. C. Loy, K. He, and X. Tang, "Image super-resolution using deep convolutional networks," IEEE Trans. on pattern analysis and machine intelligence, vol. 38, no. 2, pp. 295–307, 2015.

[2] C. Ledig, L. Theis, F. Huszár, J. Caballero, A. Cunningham, A. Acosta, A. Aitken, A. Tejani, J. Totz, Z. Wang et al., "Photo-realistic single image super-resolution using a generative adversarial network," in CVPR, 2017.

[3] N. Sonehara, M. Kawato, S. Miyake, and K. Nakane, "Image data compression using a neural network model," International 1989 Joint Conference on Neural Networks, pp. 35–41 vol.2, 1989.

[4] S. M. G.L. Sicuranza, G. Ramponi, "Artificial neural network for image compression," Electronics Letters, vol. 26, pp. 477–479(2), March 1990.

[5] J. Jiang, "Image compression with neural networks–a survey," Sig. Process.: Image Communication, vol. 14, no. 9, pp. 737–760, 1999.

[6] I. Goodfellow, J. Pouget-Abadie, M. Mirza, B. Xu, D. Warde-Farley, S. Ozair, A. Courville, and Y. Bengio, "Generative Adversarial Nets," in Neural Info. Process. Sys., vol. 27, 2014.

[7] D. Kingma and M. Welling, "Auto-encoding variational Bayes," in Int. Conf. Learn. Representations, 2014.

[8] D. Rezende and S. Mohamed, "Variational inference with normalizing flows," in Int. Conf. Mach. Learn., 2015.

[9] H. Larochelle and I. Murray, "The Neural Autoregressive Distribution Estimator," Int. Conf. on Artificial Intelligence and Statistics, 2011.

[10] A. van den Oord, S. Dieleman, H. Zen, K. Simonyan, O. Vinyals, A. Graves, N. Kalchbrenner, A. W. Senior, and K. Kavukcuoglu, "WaveNet: A Generative Model for Raw Audio," arXiv preprint arXiv:1609.03499, 2016.

[11] K. Gregor, F. Besse, D. Jimenez Rezende, I. Danihelka, and D. Wierstra, "Towards conceptual compression," Neural Info. Process. Sys., vol. 29, pp. 3549–3557, 2016.

[12] B. J. Frey, Bayesian networks for pattern classification, data compression, and channel coding. Citeseer, 1998.

[13] J. Ballé, V. Laparra, and E. P. Simoncelli, "End-to-end Optimized Image Compression," in Int. Conf. Learn. Representations, 2017.

[14] L. Theis, W. Shi, A. Cunningham, and F. Huszár, "Lossy Image Compression with Compressive Autoencoders," in Int. Conf. Learn. Representations, 2017.

[15] A. Alemi, B. Poole, I. Fischer, J. Dillon, R. A. Saurous, and K. Murphy, "Fixing a broken elbo," in Int. Conf. Mach. Learn. PMLR, 2018, pp. 159–168.

[16] Y. Yang, R. Bamler, and S. Mandt, "Improving inference for neural image compression," in Neural Info. Process. Sys., 2020.

[17] J. Ballé, P. A. Chou, D. Minnen, S. Singh, N. Johnston, E. Agustsson, S. J. Hwang, and G. Toderici, "Nonlinear transform coding," IEEE Trans. on Special Topics in Signal Processing, vol. 15, 2021.

[18] S. Ma, X. Zhang, C. Jia, Z. Zhao, S. Wang, and S. Wang, "Image and video compression with neural networks: A review," IEEE Trans. on Circuits and Systems for Video Technology, vol. 30, no. 6, pp. 1683–1698, 2019.

[19] D. Ding, Z. Ma, D. Chen, Q. Chen, Z. Liu, and F. Zhu, "Advances in video compression system using deep neural network: a review and case studies," Proc. of the IEEE, 2021.

[20] D. Minnen and S. Singh, "Channel-wise autoregressive entropy models for learned image compression," in ICIP, 2020.

[21] ITU-T, "Recommendation ITU-T T.81: Information technology – Digital compression and coding of continuous-tone still images – Requirements and guidelines," 1992.

[22] G. Hudson, A. Léger, B. Niss, I. Sebestyén, and J. Vaaben, "JPEG-1 standard 25 years: past, present, and future reasons for a success," Journal of Electronic Imaging, vol. 27, no. 4, 2018.

[23] H. Bourlard and Y. Kamp, "Auto-association by multilayer perceptrons and singular value decomposition," Biological cybernetics, vol. 59, no. 4, pp. 291–294, 1988.

[24] D. E. Rumelhart, G. E. Hinton, and R. J. Williams, "Learning internal representations by error propagation," California Univ San Diego La Jolla Inst for Cognitive Science, Tech. Rep., 1985.

[25] D. J. Rezende, S. Mohamed, and D. Wierstra, "Stochastic back-propagation and approximate inference in deep generative models," in Int. Conf. Mach. Learn., 2014.

[26] T. M. Cover and J. A. Thomas, Elements of Information Theory. John Wiley & Sons, 2006, vol. 2.

[27] C. E. Shannon, "A Mathematical Theory of Communication," Bell System Technical Journal, vol. 27, p. 379–423, 1948.

[28] R. Clausius, Mechanical Theory of Heat. Taylor and Francis, 1850-1865.

[29] L. Boltzmann, "Vorlesungen über Gastheorie," Leipzig, 1895, 1898.

[30] D. A. Huffman, "A method for the construction of minimum-redundancy codes," Proceedings of the IRE, vol. 40, no. 9, pp. 1098–1101, 1952.

[31] J. Rissanen and G. G. Langdon, "Arithmetic coding," IBM Journal of research and development, vol. 23, no. 2, pp. 149–162, 1979.

[32] G. Martín, "Range encoding: an algorithm for removing redundancy from a digitised message," in Video and Data Recording Conference, Southampton, 1979, 1979, pp. 24–27.

[33] J. Duda, "Asymmetric numeral systems," arXiv preprint arXiv:0902.0271, 2009.

[34] R. Bamler, "Understanding Entropy Coding With Asymmetric Numeral Systems (ANS): a Statistician's Perspective," arXiv preprint arXiv:2201.01741, 2022.

[35] J. Townsend, "A tutorial on the range variant of asymmetric numeral systems," arXiv preprint arXiv:2001.09186, 2020.

[36] L. Theis, A. van den Oord, and M. Bethge, "A note on the evaluation of generative models," in Int. Conf. Learn. Representations, 2016.

[37] B. Uria, I. Murray, and H. Larochelle, "RNADE: the real-valued neural autoregressive density-estimator," in Neural Info. Process. Sys. 26, vol. 26, 2013.

[38] T. Salimans, A. Karpathy, X. Chen, and D. P. Kingma, "PixelCNN++: A pixelcnn implementation with discretized logistic mixture likelihood and other modifications," in Int. Conf. Learn. Representations, 2017.

[39] E. Hoogeboom, J. Peters, R. van den Berg, and M. Welling, "Integer discrete flows and lossless compression," in Neural Info. Process. Sys., 2019, pp. 12 134–12 144.

[40] F. Mentzer, E. Agustsson, M. Tschannen, R. Timofte, and L. Van Gool, "Practical full resolution learned lossless image compression," in CVPR, 2019.

[41] J. Ballé, D. Minnen, S. Singh, S. J. Hwang, and N. Johnston, "Variational Image Compression with a Scale Hyperprior," Int. Conf. Learn. Representations, 2018.

[42] D. Minnen, J. Ballé, and G. D. Toderici, "Joint Autoregressive and Hierarchical Priors for Learned Image Compression," in Neural Info. Process. Sys. 31, 2018.

[43] C. M. Bishop, Pattern Recognition and Machine Learning, ser. Information science and statistics, M. Jordan, J. Kleinberg, and B. Schölkopf, Eds. Springer, 2006.

[44] M. Mahoney, "Large Text Compression Benchmark." [Online]. Available: http://mattmahoney.net/dc/text.html

[45] B. Knoll, "Cmix." [Online]. Available: https://www.byronknoll.com/cmix.html

[46] S. Hochreiter and J. Schmidhuber, "Long short-term memory," Neural Computation, vol. 9, no. 8, pp. 1745–1780, 1997.

[47] F. Bellard, "Lossless Data Compression with Neural Networks," 2019.

[48] R. A. Jacobs, M. I. Jordan, S. J. Nowlan, and G. E. Hinton, "Adaptive mixtures of local experts," Neural Computation, 1991.

[49] R. Hosseini, F. Sinz, and M. Bethge, "Lower bounds on the redundancy of natural images," Vision Research, vol. 50, no. 22, pp. 2213–2222, 2010.

[50] L. Theis, R. Hosseini, and M. Bethge, "Mixtures of conditional Gaussian scale mixtures applied to multiscale image representations," PLoS ONE, vol. 7, no. 7, 2012.

[51] L. Theis and M. Bethge, "Generative image modeling using spatial LSTMs," in Neural Info. Process. Sys. 28, 2015.

[52] A. van den Oord, N. Kalchbrenner, O. Vinyals, A. G. L. Espeholt, and K. Kavukcuoglu, "Conditional Image Generation with PixelCNN Decoders," in Neural Info. Process. Sys, 2016.

[53] N. Parmar, A. Vaswani, J. Uszkoreit, L. Kaiser, N. Shazeer, A. Ku, and D. Tran, "Image transformer," in Int. Conf. Mach. Learn., 2018.

[54] A. Vaswani, N. Shazeer, N. Parmar, J. Uszkoreit, L. Jones, A. N. Gomez, L. Kaiser, and I. Polosukhin, "Attention is all you need," in Neural Info. Process. Sys., vol. 30, 2017, pp. 5998–6008.

[55] X. Chen, N. Mishra, M. Rohaninejad, and P. Abbeel, "PixelSNAIL: An improved autoregressive generative model," in Int. Conf. Mach. Learn., 2018.

[56] D. P. Kingma and P. Dhariwal, "Glow: Generative Flow with Invertible 1x1 Convolutions," in Neural Info. Process. Sys. 31, S. Bengio, H. Wallach, H. Larochelle, K. Grauman, N. Cesa-Bianchi, and R. Garnett, Eds., 2018, pp. 10 215–10 224.

[57] X. Wu, K. U. Barthel, and W. Zhang, "Piecewise 2D Autoregression for Predictive Image Coding," in ICIP. IEEE Computer Society, 1998, pp. 901–904.

[58] B. Meyer and P. Tischer, "Glicbawls – Grey Level Image Compression By Adaptive Weighted Least Squares," in Data Compression Conference, 2001.

[59] M. Stern, N. Shazeer, and J. Uszkoreit, "Blockwise parallel decoding for deep autoregressive models," in Neural Info. Process. Sys., vol. 31, 2018.

[60] C. Zhang, J. Bütepage, H. Kjellström, and S. Mandt, "Advances in variational inference," IEEE Trans. on pattern analysis and machine intelligence, vol. 41, no. 8, pp. 2008–2026, 2018.

[61] P. D. Grünwald, The minimum description length principle. MIT press, 2007.

[62] C. S. Wallace, "Classification by minimum-message-length inference," in Int. Conf. on Computing and Information. Springer, 1990, pp. 72–81.

[63] A. Honkela and H. Valpola, "Variational learning and bits-back coding: an information-theoretic view to bayesian learning," IEEE Trans. on Neural Networks, vol. 15, no. 4, pp. 800–810, 2004.

[64] B. J. Frey and G. E. Hinton, "Efficient stochastic source coding and an application to a bayesian network source model," The Computer Journal, vol. 40, no. 2_and_3, pp. 157–165, 1997.

[65] G. E. Hinton and D. Van Camp, "Keeping the neural networks simple by minimizing the description length of the weights," in Proc. of the 6th Conf. on Comp. Learn. Theory, 1993, pp. 5–13.

[66] J. Townsend, T. Bird, and D. Barber, "Practical lossless compression with latent variables using bits back coding," arXiv preprint arXiv:1901.04866, 2019.

[67] D. J. MacKay and D. J. Mac Kay, Information theory, inference and learning algorithms. Cambridge university press, 2003.

[68] J. Ho, E. Lohn, and P. Abbeel, "Compression with flows via local bits-back coding," in Neural Info. Process. Sys., 2019.

[69] J. Townsend, T. Bird, J. Kunze, and D. Barber, "Hilloc: Lossless image compression with hierarchical latent variable models," arXiv preprint arXiv:1912.09953, 2019.

[70] Y. Ruan, K. Ullrich, D. Severo, J. Townsend, A. Khisti, A. Doucet, A. Makhzani, and C. J. Maddison, "Improving lossless compression rates via monte carlo bits-back coding," in Int. Conf. Mach. Learn., 2021.

[71] J. Townsend and I. Murray, "Lossless compression with state space models using bits back coding," arXiv preprint arXiv:2103.10150, 2021.

[72] C. Cremer, X. Li, and D. Duvenaud, "Inference suboptimality in variational autoencoders," in Int. Conf. Mach. Learn., 2018.

[73] Y. Burda, R. Grosse, and R. Salakhutdinov, "Importance weighted autoencoders," arXiv preprint arXiv:1509.00519, 2015.

[74] L. Theis and J. Ho, "Importance weighted compression," in Neural Compression Workshop at ICLR 2021, 2021.

[75] D. Tran, K. Vafa, K. Agrawal, L. Dinh, and B. Poole, "Discrete flows: Invertible generative models of discrete data," in Neural Info. Process. Sys., 2019, pp. 14 719–14 728.

[76] A. Liu, S. Mandt, and G. V. d. Broeck, "Lossless compression with probabilistic circuits," in Int. Conf. Learn. Representations, 2022.

[77] J. Sohl-Dickstein, E. Weiss, N. Maheswaranathan, and S. Ganguli, "Deep unsupervised learning using nonequilibrium thermodynamics," in Int. Conf. Mach. Learn. PMLR, 2015, pp. 2256–2265.

[78] E. Hoogeboom, A. A. Gritsenko, J. Bastings, B. Poole, R. v. d. Berg, and T. Salimans, "Autoregressive diffusion models," arXiv preprint arXiv:2110.02037, 2021.

[79] C. Shannon, "Coding theorems for a discrete source with a fidelity criterion," IRE Nat. Conv. Rec., March 1959, vol. 4, pp. 142–163, 1959.

[80] Y. Yang, , and S. Mandt, "Towards empirical sandwich bounds on the rate-distortion function," in Int. Conf. Learn. Representations, 2022.

[81] P. A. Chou, T. Lookabaugh, and R. M. Gray, "Entropy-constrained vector quantization," IEEE Trans. on Acoustics, Speech, and Sig. Process., vol. 37, no. 1, pp. 31–42, 1989.

[82] J. Degrave and I. Korshunova, "How we can make machine learning algorithms tunable." [Online]. Available: https://www.engraved.blog/how-we-can-make-machine-learning-algorithms-tunable/

[83] J. C. Platt and A. H. Barr, "Constrained differential optimization for neural networks," California Institute of Technology, Tech. Rep., 1988.

[84] T. van Rozendaal, G. Sautière, and T. S. Cohen, "Lossy compression with distortion constrained optimization," 2020.

[85] J. Ziv, "On universal quantization," IEEE Trans. on Info. Theory, vol. 31, no. 3, pp. 344–347, 1985.

[86] G. J. Sullivan, "Efficient scalar quantization of exponential and laplacian random variables," IEEE Trans. on Info. Theory, vol. 42, no. 5, pp. 1365–1374, 1996.

[87] S. Lloyd, "Least squares quantization in pcm," IEEE Trans. on Info. Theory, vol. 28, no. 2, pp. 129–137, 1982.

[88] A. Gersho and R. M. Gray, Vector quantization and signal compression. Springer Science & Business Media, 2012, vol. 159.

[89] K. Sayood, "Vector quantization," in Introduction to Data Compression, 4th ed., K. Sayood, Ed. Morgan Kaufmann, 2012.

[90] V. K. Goyal, "Theoretical foundations of transform coding," IEEE Sig. Process. Magazine, vol. 18, no. 5, pp. 9–21, 2001.

[91] I. Goodfellow, Y. Bengio, and A. Courville, Deep learning. MIT press, 2016.

[92] J. Ballé, V. Laparra, and E. P. Simoncelli, "End-to-end optimization of nonlinear transform codes for perceptual quality," in Picture Coding Symposium, 2016.

[93] G. Toderici, D. Vincent, N. Johnston, S. Jin Hwang, D. Minnen, J. Shor, and M. Covell, "Full resolution image compression with recurrent neural networks," in CVPR, 2017.

[94] N. Johnston, E. Eban, A. Gordon, and J. Ballé, "Computationally efficient neural image compression," arXiv preprint arXiv:1912.08771, 2019.

[95] T. G. Bever and D. Poeppel, "Analysis by synthesis: a (re-) emerging program of research for language and vision," Biolinguistics, vol. 4, no. 2-3, pp. 174–200, 2010.

[96] G. Toderici, S. M. O'Malley, S. J. Hwang, D. Vincent, D. Minnen, S. Baluja, M. Covell, and R. Sukthankar, "Variable rate image compression with recurrent neural networks," in Int. Conf. Learn. Representations, 2016.

[97] R. J. Williams, "Simple statistical gradient-following algorithms for connectionist reinforcement learning," Machine learning, vol. 8, no. 3, pp. 229–256, 1992.

[98] Y. Bengio, N. Leonard, and A. Courville, "Estimating or propagating gradients through stochastic neurons for conditional computation," arXiv preprint arXiv:1308.3432, 2013.

[99] M. Li, W. Zuo, S. Gu, D. Zhao, and D. Zhang, "Learning convolutional networks for content-weighted image compression," arXiv preprint arXiv:1703.10553, 2017.

[100] E. Agustsson, F. Mentzer, M. Tschannen, L. Cavigelli, R. Timofte, L. Benini, and L. V. Gool, "Soft-to-Hard Vector Quantization for End-to-End Learning Compressible Representations," in Neural Info. Process. Sys. 30, 2017, pp. 1141–1151.

[101] F. Mentzer, E. Agustsson, M. Tschannen, R. Timofte, and L. Van Gool, "Conditional probability models for deep image compression," in CVPR, 2018.

[102] E. Agustsson and L. Theis, "Universally Quantized Neural Compression," in Neural Info. Process. Sys., 2020.

[103] A. Habibian, T. v. Rozendaal, J. M. Tomczak, and T. S. Cohen, "Video compression with rate-distortion autoencoders," in CVPR, 2019.

[104] E. Jang, S. Gu, and B. Poole, "Categorical reparameterization with gumbel-softmax," arXiv preprint arXiv:1611.01144, 2016.

[105] C. J. Maddison, A. Mnih, and Y. W. Teh, "The concrete distribution: A continuous relaxation of discrete random variables," arXiv preprint arXiv:1611.00712, 2016.

[106] K. Tsubota and K. Aizawa, "Comprehensive comparisons of uniform quantizers for deep image compression," in ICIP, 2021, pp. 2089–2093.

[107] J. Lee, S. Cho, and S.-K. Beack, "Context-adaptive entropy model for end-to-end optimized image compression," in Int. Conf. Learn. Representations, 2019.

[108] E. Agustsson, D. Minnen, N. Johnston, J. Balle, S. J. Hwang, and G. Toderici, "Scale-space flow for end-to-end optimized video compression," in CVPR, 2020.

[109] Y. Choi, M. El-Khamy, and J. Lee, "Variable rate deep image compression with a conditional autoencoder," in ICCV, 2019.

[110] J. Ballé, N. Johnston, and D. Minnen, "Integer networks for data compression with latent-variable models," in Int. Conf. Learn. Representations, 2018.

[111] Y. Yang, R. Bamler, and S. Mandt, "Variational Bayesian Quantization," in Int. Conf. Mach. Learn., 2020.

[112] C. H. Bennett and P. W. Shor, "Entanglement-Assisted Capacity of a Quantum Channel and the Reverse Shannon Theorem," IEEE Trans. on Info. Theory, vol. 48, no. 10, 2002.

[113] R. Zamir, Lattice Coding for Signals and Networks. Cambridge University Press, 2014.

[114] C. T. Li and A. E. Gamal, "Strong Functional Representation Lemma and Applications to Coding Theorems," in IEEE Int. Symposium on Information Theory, 2017.

[115] G. Flamich, M. Havasi, and J. M. Hernández-Lobato, "Compressing Images by Encoding Their Latent Representations with Relative Entropy Coding," 2020, neural Info. Process. Sys. 34.

[116] L. Theis and N. Yosri, "Algorithms for the communication of samples," arXiv preprint arXiv:2110.12805, 2021.

[117] L. G. Roberts, "Picture Coding Using Pseudo-Random Noise," IRE Trans. on Info. Theory, 1962.

[118] R. Zamir and M. Feder, "On universal quantization by randomized uniform/lattice quantizers," IEEE Trans. on Info. Theory, vol. 38, no. 2, pp. 428–436, 1992.

[119] P. Harsha, R. Jain, D. McAllester, and J. Radhakrishnan, "The Communication Complexity of Correlation," in 22nd Annual IEEE Conference on Computational Complexity, 2007, pp. 10–23.

[120] P. Cuff, "Communication requirements for generating correlated random variables," in 2008 IEEE Int. Symposium on Information Theory, 2008, pp. 1393–1397.

[121] P. W. Cuff and E. C. Song, "The likelihood encoder for source coding," in 2013 IEEE Information Theory Workshop, 2013.

[122] M. Havasi, R. Peharz, and J. M. Hernández-Lobato, "Minimal Random Code Learning: Getting Bits Back from Compressed Model Parameters," in Int. Conf. Learn. Representations, 2019.

[123] E. C. Song, P. Cuff, and H. V. Poor, "The likelihood encoder for lossy compression," IEEE Trans. on Info. Theory, vol. 62, 2016.

[124] L. Theis and E. Agustsson, "On the advantages of stochastic encoders," arXiv preprint arXiv:2102.09270, 2021.

[125] ITU-T, "Recommendation ITU-T T.800.2: Methods for objective and subjective assessment of speech and video quality," 2016.

[126] K. Storrs, S. V. Leuven, S. Kojder, L. Theis, and F. Huszár, "Adaptive paired-comparison method for subjective video quality assessment on mobile devices," in Picture Coding Symposium, 2018.

[127] T.-J. Liu, Y.-C. Lin, W. Lin, and C.-C. J. Kuo, "Visual quality assessment: recent developments, coding applications and future trends," APSIPA Trans. on Signal and Info. Processing, 2013.

[128] Z. Li, A. Aaron, I. Katsavounidis, A. Moorthy, and M. Manohara, "Toward a practical perceptual video quality metric," 2016, netflix Technology Blog. [Online]. Available: https://netflixtechblog.com/toward-a-practical-perceptual-video-quality-metric-653f208b9652

[129] A. M. Eskicioglu and P. S. Fisher, "Image quality measures and their performance," IEEE Trans. on Communications, vol. 43, pp. 2959 – 2965, 1995.

[130] Zhou Wang, A. C. Bovik, H. R. Sheikh, and E. P. Simoncelli, "Image quality assessment: from error visibility to structural similarity," IEEE Trans. on Image Processing, vol. 13, no. 4, pp. 600–612, 2004.

[131] Z. Wang, E. P. Simoncelli, and A. C. Bovik, "Multiscale structural similarity for image quality assessment," in 37th Asilomar Conference on Signals, Systems Computers, 2003, vol. 2, 2003.

[132] C. Ledig, L. Theis, F. Huszar, J. Caballero, A. Cunningham, A. Acosta, A. Aitken, A. Tejani, J. Totz, Z. Wang, and W. Shi, "Photo-realistic single image super-resolution using a generative adversarial network," in CVPR, 2017.

[133] F. Mentzer, G. D. Toderici, M. Tschannen, and E. Agustsson, "High-fidelity generative image compression," Neural Info. Process. Sys., vol. 33, 2020.

[134] M. Strathern, "Improving ratings: audit in the British University system," European Review, vol. 5, pp. 305–321, 1997.

[135] K. Ding, K. Ma, S. Wang, and E. P. Simoncelli, "Comparison of Full-Reference Image Quality Models for Optimization of Image Processing Systems," International Journal of Computer Vision, no. 129, pp. 1258–1281, 2021.

[136] L. A. Gatys, A. S. Ecker, and M. Bethge, "Image style transfer using convolutional neural networks," in CVPR, 2016.

[137] J. Bruna, P. Sprechmann, and Y. LeCun, "Super-resolution with deep convolutional sufficient statistics," in Int. Conf. Learn. Representations, 2016.

[138] K. Simonyan and A. Zisserman, "Very deep convolutional networks for large-scale image recognition," in Int. Conf. Learn. Representations, 2015.

[139] J. Bruna and S. Mallat, "Invariant scattering convolution networks," IEEE Trans. on Pattern Analysis and Machine Intelligence, vol. 35, no. 8, pp. 1872–1886, 2013.

[140] R. Zhang, P. Isola, A. A. Efros, E. Shechtman, and O. Wang, "The Unreasonable Effectiveness of Deep Features as a Perceptual Metric," in CVPR, 2018.

[141] A. Krizhevsky, I. Sutskever, and G. E. Hinton, "Imagenet classification with deep convolutional neural networks," in Neural Info. Process. Sys., 2012.

[142] S. Bhardwaj, I. Fischer, J. Ballé, and T. Chinen, "An Unsupervised Information-Theoretic Perceptual Quality Metric," in Neural Info. Process. Sys., vol. 33, 2020, pp. 13–24.

[143] A. Mittal, R. Soundararajan, and A. C. Bovik, "Making a "Completely Blind" Image Quality Analyzer," IEEE Signal Processing Letters, vol. 20, no. 3, pp. 209–212, Mar. 2013.

[144] L. Zhang, L. Zhang, and A. C. Bovik, "A feature-enriched completely blind image quality evaluator," IEEE Trans. on Image Processing, vol. 24, no. 8, pp. 2579–2591, 2015.

[145] S. Bosse, D. Maniry, T. Wiegand, and W. Samek, "A deep neural network for image quality assessment," in ICIP, 2016, pp. 3773–3777.

[146] H. Sheikh, M. Sabir, and A. Bovik, "A statistical evaluation of recent full reference image quality assessment algorithms," IEEE Trans. on Image Processing, vol. 15, no. 11, pp. 3440–3451, 2006.

[147] J. Kim, A.-D. Nguyen, and S. Lee, "Deep cnn-based blind image quality predictor," IEEE Trans. on Neural Networks and Learning Systems, vol. 30, no. 1, pp. 11–24, 2019.

[148] T. Minka, "Divergence measures and message passing," Microsoft Research, Tech. Rep. TR-2005-173, 2005.

[149] S. Nowozin, B. Cseke, and R. Tomioka, "f-GAN: Training Generative Neural Samplers using Variational Divergence Minimization," in Neural Info. Process. Sys., vol. 29, 2016.

[150] O. Rippel and L. Bourdev, "Real-time adaptive image compression," in Int. Conf. Mach. Learn., 2017.

[151] S. Santurkar, D. Budden, and N. Shavit, "Generative compression," in Picture Coding Symposium, 2018.

[152] E. Agustsson, M. Tschannen, F. Mentzer, R. Timofte, and L. V. Gool, "Generative adversarial networks for extreme learned image compression," in ICCV, 2019.

[153] X. Mao, Q. Li, H. Xie, R. Y. K. Lau, Z. Wang, and S. P. Smolley, "Least squares generative adversarial networks," in ICCV, 2017, pp. 2813–2821.

[154] B. Poole, A. Alemi, J. Sohl-dickstein, and A. Angelova, "Improved generator objectives for GANs," arXiv preprint arXiv:1612.02780, 2016.

[155] M. Heusel, H. Ramsauer, T. Unterthiner, B. Nessler, and S. Hochreiter, "GANs Trained by a Two Time-Scale Update Rule Converge to a Local Nash Equilibrium," in Neural Info. Process. Sys., vol. 30, 2017.

[156] C. Szegedy, V. Vanhoucke, S. Ioffe, J. Shlens, and Z. Wojna, "Rethinking the inception architecture for computer vision," arXiv, vol. 1512.00567, 2015.

[157] Y. Blau and T. Michaeli, "The perception-distortion tradeoff," in CVPR, 2018.

[158] A. Dosovitskiy and T. Brox, "Generating images with perceptual similarity metrics based on deep networks," in Neural Info. Process. Sys., vol. 29, 2016.

[159] F. Yang, H. Talebi, M. Elad, P. Milanfar, and X. Luo, "The rate-distortion-accuracy tradeoff: Jpeg case study," in Proc. of the Data Compression Conference, 2020.

[160] S. Singh, S. Abu-El-Haija, N. Johnston, J. Ballé, A. Shrivastava, and G. Toderici, "End-to-end learning of compressible features," in ICIP. IEEE, 2020, pp. 3349–3353.

[161] Y. Matsubara, R. Yang, M. Levorato, and S. Mandt, "Supervised compression for resource-constrained edge computing systems," arXiv preprint arXiv:2108.11898, 2021.

[162] Y. Dubois, B. Bloem-Reddy, K. Ullrich, and C. J. Maddison, "Lossy compression for lossless prediction," in Neural Info. Process. Sys., 2021.

[163] B. Rajesh, M. Javed, Ratnesh, and S. Srivastava, "Dct-compcnn: A novel image classification network using jpeg compressed dct coefficients," in 2019 IEEE Conference on Information and Communication Technology, 2019, pp. 1–6.

[164] T. Chen, H. Liu, Q. Shen, T. Yue, X. Cao, and Z. Ma, "Deepcoder: A deep neural network based video compression," in 2017 IEEE Visual Communications and Image Processing (VCIP). IEEE, 2017, pp. 1–4.

[165] C.-Y. Wu, N. Singhal, and P. Krahenbuhl, "Video compression through image interpolation," in Proc. of the European Conference on Computer Vision, 2018, pp. 416–431.

[166] A. Djelouah, J. Campos, S. Schaub-Meyer, and C. Schroers, "Neural inter-frame compression for video coding," in ICCV, 2019.

[167] J. Han, S. Lombardo, C. Schroers, and S. Mandt, "Deep generative video compression," in Neural Info. Process. Sys., 2019.

[168] G. Lu, W. Ouyang, D. Xu, X. Zhang, C. Cai, and Z. Gao, "Dvc: An end-to-end deep video compression framework," in CVPR, 2019.

[169] A. Golinski, R. Pourreza, Y. Yang, G. Sautiere, and T. S. Cohen, "Feedback recurrent autoencoder for video compression," in Proc. of the Asian Conference on Computer Vision, 2020.

[170] R. Yang, F. Mentzer, L. Van Gool, and R. Timofte, "Learning for video compression with recurrent auto-encoder and recurrent probability model," IEEE Journal of Selected Topics in Signal Processing, 2020.

[171] G. Lu, X. Zhang, W. Ouyang, L. Chen, Z. Gao, and D. Xu, "An end-to-end learning framework for video compression," IEEE Trans. on pattern analysis and machine intelligence, 2020.

[172] A. Dosovitskiy, P. Fischer, E. Ilg, P. Hausser, C. Hazirbas, V. Golkov, P. Van Der Smagt, D. Cremers, and T. Brox, "Flownet: Learning optical flow with convolutional networks," in ICCV, 2015.

[173] O. Rippel, S. Nair, C. Lew, S. Branson, A. G. Anderson, and L. Bourdev, "Learned video compression," in ICCV, 2019.

[174] R. Yang, Y. Yang, J. Marino, and S. Mandt, "Hierarchical autoregressive modeling for neural video compression," in Int. Conf. Learn. Representations, 2020.

[175] L. Dinh, D. Krueger, and Y. Bengio, "Nice: Non-linear independent components estimation," arXiv preprint arXiv:1410.8516, 2014.

[176] L. Dinh, J. Sohl-Dickstein, and S. Bengio, "Density estimation using real nvp," arXiv preprint arXiv:1605.08803, 2016.

[177] L. Zhou, C. Cai, Y. Gao, S. Su, and J. Wu, "Variational Autoencoder for Low Bit-rate Image Compression," in Challenge on Learned Image Compression, 2018.

Yibo Yang is a Ph.D. candidate at the University of California, Irvine. His research interests include probability theory, information theory, and their applications in machine learning. He regularly serves as a reviewer for ICML, NeurIPS, and ICLR, and has received multiple best reviewer awards. His research is supported by a fellowship from the Hasso Plattner Institute.

Stephan Mandt is an Assistant Professor of Computer Science and Statistics at the University of California, Irvine. From 2016 until 2018, he was a Senior Researcher and Head of the statistical machine learning group at Disney Research. He held previous postdoctoral positions at Columbia University and Princeton University. Stephan holds a Ph.D. in Theoretical Physics from the University of Cologne, where he received the German National Merit Scholarship. He is furthermore a Kavli Fellow of the U.S. National Academy of Sciences and an NSF CAREER Awardee. Stephan regularly serves as an Area Chair or Editorial Board member for NeurIPS, ICML, AAAI, ICLR, and JMLR. His research is currently supported by NSF, DARPA, DOE, Intel, Disney, and Qualcomm.

Lucas Theis is a senior research scientist at Google where he works on neural compression and information theory. He previously worked for Magic Pony Technologies, a London based neural compression startup which got acquired by Twitter in 2016. At Twitter, he worked on compression, super-resolution, and other topics until 2019. Lucas obtained his PhD degree (summa cum laude) in 2016 from the Max Planck Research School in Tübingen, Germany for his work on deep generative image models.